Uniqueness of Power Flow Solutions Using Monotonicity and Network Topology

SangWoo Park, Richard Y. Zhang, Javad Lavaei and Ross Baldick

***Abstract*—This paper establishes sufficient conditions for the uniqueness of AC power flow solutions via the monotonic relationship between real power flow and the phase angle difference. More specifically, we prove that the $P-\Theta$ power flow problem has at most one solution for any acyclic or *GSP* graph. In addition, for arbitrary cyclic power networks, we show that multiple distinct solutions cannot exist under the assumption that angle differences across the lines are bounded by some limit related to the maximal girth of the network. In these cases, a vector of voltage phase angles can be uniquely determined (up to an absolute phase shift) given a vector of real power injections within the realizable range. The implication of this result for classical power flow analysis is that, under the conditions specified above, the problem has a unique physically realizable solution if the phasor voltage magnitudes are fixed. We also introduce a series-parallel operator and show that this operator obtains a reduced and easier-to-analyze model for the power system without changing the uniqueness of power flow solutions.**

I. INTRODUCTION

The AC power flow equations fundamentally underpin every aspect of power systems: from day-to-day operations in contingency analysis, security-constrained dispatch of electricity markets and yearly capacity planning for peak load, to decades-long transmission expansion and renewable integration. The purpose of AC power flow problem is to solve for the complex voltages, described by their magnitudes and phase angles, given a power system set-point. The power flow equations are nonlinear, and may admit multiple solutions. In the past, the conventional wisdom was to assume that the solution becomes unique by restricting it to "realistic" or "physically realizable" values. However, various examples in the literature show that multiple solutions may persist even after restricting either voltage magnitudes or phase angle differences to "physically realizable" values [2], [3], [4, Section IV]. For the former, we present an example in Section V where multiple solutions exist despite having fixed voltage magnitudes for all buses. For the latter, it is possible to construct a two-bus example — one slack bus and one PQ bus — that admits a high-voltage solution within standard operating limits, and another low-voltage solution with a large phase angle difference of 49.9 degrees that is still below the steady-state limit of 90 degrees [5]. Therefore, in principle, system operators may encounter operating points that are very different from what they had expected. In order to avoid these situations, it is important to understand whether or not there is a unique "physically realizable" power flow solution for real-world power systems. The goal of this paper is to develop sufficient conditions on top of the "realism" that will guarantee a unique solution to the AC power flow equations.

SangWoo Park and Javad Lavaei are with the Department of Industrial Engineering and Operations Research, University of California Berkeley. Emails: { spark111, lavaei }@berkeley.edu. Richard Y. Zhang is with the Department of Electrical and Computer Engineering, University of Illinois at Urbana-Champaign. Email: ryz@illinois.edu. Ross Baldick is with the Department of Electrical and Computer Engineering, University of Texas at Austin. Email: baldick@ece.utexas.edu.

The authors affiliated with UC Berkeley were in part supported by the ARO grant W911NF-17-1-0555, NSF Awards 1808859 and 1807260. Ross Baldick was in part supported by the University of Texas Faculty Development Program. Parts of this paper have appeared in the conference paper [1].

A. Monotonicity between phase angles and power flow

Mathematical tools that are often used to prove uniqueness results include the fixed point theorem with contraction mapping and the inverse function theorem. In this paper, we use the notion of monotonicity to prove uniqueness of the power flow solution under certain conditions. The results that we present stem from a simple idea that is best explained via an example. Consider a two-bus, lossless one-line system, with the line reactance X. Voltage magnitude and angle are specified at one of the buses ("slack bus"), whereas real power injection and voltage magnitude are specified at the other bus ("PV bus"). Then, the power transfer between the two buses is given with respect to the two voltage magnitudes $|v_1|, |v_2|$ and the angular difference $\theta_1-\theta_2$ as a sinusoid: $P=|v_1|\cdot|v_2|\cdot\sin(\theta_1-\theta_2)/X$.

Even in this simple toy example, we can see that the power flow solutions are not unique: every value of P satisfying $|P|< |v_1|\cdot|v_2|/X$ can be attained by two choices of $\theta_1-\theta_2$. However, if we restrict $\theta_1-\theta_2$ to take on what we will call *physically realizable* values within the steady-state stability limit of $|\theta_1-\theta_2|< \pi/2$, then the solution becomes unique. Indeed, this follows from the fact that P is *monotonically increasing* with respect to $\theta_1-\theta_2$ within this range. Formally, if we define $f(x)=(|v_1|\cdot|v_2|/X)\sin x$ as the power flow function and $\Omega=[-\pi/2,+\pi/2]$ as the range of acceptable values for x, then the strictly increasing property of f guarantees the following inequality:

$$(f(x)-f(y))(x-y)>0 \quad \forall x\neq y, \quad x,y\in\Omega.$$

The inequality forces the nonlinear equation $f(x)=P$ to have no more than one solution $x\in\Omega$, because a different $y\in\Omega$ satisfying $f(y)=P$ would contradict the inequality. Hence, the phase angles θ_1 and θ_2 can be uniquely determined (up to an absolute phase shift) given a value of P within the realizable range $|P|< |v_1|\cdot|v_2|/X$. This paper extends this idea to an arbitrary power network using a multi-dimensional generalization of the monotonicity property.

B. Main results

The major contribution of this paper is the identification of sufficient conditions under which the power flow equations have a unique "realistic" solution. For the remainder of the paper, we focus on the relationship between voltage angle differences and real power injections, referred to as the $P-\Theta$ problem in the literature [6]. Analogous to the two-bus case, a set of phase angles are *physically realizable* for a lossless system if the angular difference across every line lies within the stability limit of $\pi/2$. Under the constraint that phase angles are *physically realizable* and smaller than a certain limit that depends on the network topology, we extend the notion of monotonicity that was illustrated for the earlier two-bus example to high-dimensional networks. The contributions of this paper are summarized below:

- We show that all acyclic networks have at most one $P-\Theta$ power flow solution under certain conditions on voltage angles. Furthermore, the set of feasible real power injections (for non-slack buses) on these graphs is a convex set.
- We show that cyclic networks cannot have multiple distinct $P-\Theta$ power flow solutions under certain conditions on voltage angles. These conditions can be checked offline and provide a certificate for ruling out multiple solutions. The certificate is easier to satisfy for graphs with smaller *maximal girth*.
- We show that the uniqueness of $P-\Theta$ power flow solutions is preserved under series-parallel reduction. A natural corollary to this is that power systems with *Generalized Series-Parallel graphs* have at most one $P-\Theta$ power flow solution under some angle conditions. Loosely speaking, these are graphs that can be constructed entirely out of series and parallel terminal connections in circuit theory, plus dangling vertices. Any tree or cycle graph is a Generalized Series-Parallel graph.

The implication of these results for classical power flow analysis is that, under the conditions specified above, the problem has a unique physically realizable solution if the phasor voltage magnitudes are fixed. This occurs, for example, if all buses except the slack bus are modeled as PV buses. In practice, tightly controlled voltage magnitudes are enforced by operating limits, and are usually achieved through the availability of dispersed and controllable reactive sources. The assumption is commonly used in the power industry and is implicit in the DC power flow equations.

C. Related work

The paper [7] is one of the first to study the solution set of the power flow equations, which contrary to the conjecture at that time constructed an example showing the general non-uniqueness of decoupled power flow solutions. A more thorough study was later presented in the paper [8], which derived the estimate number of solutions and characterized the stability region for the power flow problem. However, the results are limited to lossless transmission networks consisting of only PV buses. Soon after, [9] formulated the coupled power flow equations in rectangular coordinates and described a set of linear necessary conditions for the solution of the power flow problem, which helped systematically investigate the problem feasibility. Subsequently, researchers have tried to explicitly characterize conditions under which the power flow solution exists and is unique. For example, the work [10] derived conditions under which the reactive power-voltage problem has a unique solution under decoupling assumptions. Then, [6] extended these results by deriving conditions for the real power-phase angle problem under the same decoupling assumptions. Note that in this paper, we consider the real power-phase angle problem as in [6], but discard the decoupling assumptions because it fails to accurately capture the true physics when transmission lines are not purely inductive. Furthermore, we consider a general lossy network.

Researchers have also observed that information about the topology of the power system network can be utilized to derive stronger results. Without making decoupling assumptions, the paper [2] investigated the number of power flow solutions in a radial network and showed that, for practical system parameters, the solution always exists and is unique. The results were extended to unbalanced three-phase distribution networks in [11]. Adding to these results, the work in [12] shows that several algorithms, using the fixed-point, convex relaxation and the energy function approaches, converge to the unique high-voltage solution for radial networks. In the more recent study [13], the authors studied the power flow problem and its relationship to optimization in tree networks by mainly analyzing the injection region of the power network. While these results are limited to tree graphs, our current work characterizes a wider class of topologies under which the power flow solution is unique. Finally, the work in [14] used the network topology to upper bound the number of power flow solutions.

The most widely used tool to prove existence and uniqueness of power flow solutions is the fixed point technique. The work [15] was the first to apply the fixed point technique developed for nonlinear circuits to power flow. In [16] and [17], a fixed point formulation of the power flow problem was used to specify a domain around a feasible point and derive sufficient conditions for a unique solution. In the recent works [18] and [19], the authors developed a new fixed point formulation of the lossless power flow equations that includes both PQ and PV buses, and for radial networks derived network parametric conditions that guarantee the existence and uniqueness of a high-voltage solution. Extensions of the conditions to multi-phase distribution systems appear in [20] and new sufficient conditions using a fixed point technique on the complex domain appear in [21].

Moving away from fixed point techniques, the work [22] developed a semidefinite programming based procedure to characterize the domain of voltages over which the power flow operator is monotone. In a similar but different spirit, this paper utilizes monotonicity to rule out multiple solutions. Furthermore, we take advantage of the network topology information to derive less conservative sufficient conditions. The recent work [23] presents a unifying framework for network problems on the n-torus while introducing the concept of *winding cell* that is used to partition solutions. The framework can be applied to the AC power flow problem under the lossless setting and their monotonicity assumptions share close resemblance to our approach. In this work, we provide a more general result on arbitrary networks with losses.

The remainder of this paper is organized as follows. Section II lays out the basic notations used in this paper. In Section III, we define the $P-\Theta$ power flow problem formulation. Section IV establishes the condition under which strict monotonicity holds over a single line and presents favorable properties that arise from the monotonicity. The properties are used to prove that there is at most one power flow solution for acyclic networks. Section V extends this result to general cyclic networks. We present additional (voltage) angular conditions under which cyclic graphs cannot have multiple distinct power flow solutions. This condition is closely related to the *maximal girth* of the underlying graph. Section VI shows that series-parallel reduction on a graph preserves the uniqueness of power flow solutions, and arrive at the conclusion that *Generalized Series-Parallel* networks have at most one solution under additional angle constraints. Section VII develops a linear-time algorithm for a subset of *Generalized Series-Parallel* graphs. Finally, Section VIII provides numerical and simulation results that support the ideas developed in the paper. All the proofs will be delineated in the Appendix.

II. NOTATIONS

We start with some mathematical notations. For a given vector x, let x_k denote its k-th element. When notation is overloaded, $x(k)$ will sometimes take on the role of x_k. The symbol $\mathbf{j}$ denotes the unit imaginary number. The notations $(\cdot)^T$ and $(\cdot)^H$ denote the transpose and Hermitian transpose of a matrix, respectively. For a complex number z, $|z|$ denotes its magnitude and for a set X, the symbol $|X|$ denotes its cardinality. $\Re(\cdot)$ denotes the real part of a given argument.

Power system topology is specified by an undirected graph $\mathbb{G} = (\mathbb{V}, \mathbb{E})$ and we assume that this graph is simple and connected. For an undirected graph $\mathbb{G} = (\mathbb{V}, \mathbb{E})$, $\mathbb{V}$ is the set of vertices (buses) and $\mathbb{E} \subseteq \mathbb{V} \times \mathbb{V}$ is the set of undirected edges (lines). If the edges of an undirected graph are weighted with the weights captured by a set $\mathbb{W}$, then the graph is represented as $\mathbb{G} = (\mathbb{V}, \mathbb{E}, \mathbb{W})$. For a directed graph (digraph) $\mathbb{D} = (\mathbb{V}, \widetilde{\mathbb{E}}, \mathbb{W})$, $\widetilde{\mathbb{E}} \subseteq \mathbb{V} \times \mathbb{V}$ denotes the set of directed edges. The undirected edge e connecting two vertices k and ℓ is denoted by a set notation $e = \{k, \ell\}$, whereas $a = (k, \ell)$ denotes a directed edge a coming out of vertex k and going into ℓ. Depending on the context, an edge can be denoted by either e or $\{k, \ell\}$. The same goes for directed edges. The series element of the equivalent Π-model of each line $\{k, \ell\}$ is modeled by admittance $G_{k\ell} - \mathbf{j}B_{k\ell}$, where $G_{k\ell}, B_{k\ell} \geq 0$. Let d denote the vector of degrees, where its k-th element $d(k)$ stands for the degree of vertex $k \in \mathbb{V}$. Similarly, limited to directed graphs, let d^+ and d^- denote the vectors of out-degrees and in-degrees, respectively. Moreover, let $\mathbb{G}[\mathbb{V}']$ and $\mathbb{E}[\mathbb{V}']$ denote the subgraph and edge-subset of $\mathbb{G}$ that are induced by a given vertex set $\mathbb{V}' \subseteq \mathbb{V}$, respectively. The symbol $\mathbf{1}$ is the vector of ones. Finally, K_n denotes the complete graph on n vertices.

III. P-Θ PROBLEM FORMULATION

As mentioned in the introduction, we focus our attention to the relationship between the voltage phasor angles and the real power injections. To this end, we will study the mapping from angles to real powers. Let the slack bus (also the reference bus) be indexed by 1, unless defined otherwise. Let $v \in \mathbb{C}^n$ be the vector of complex bus voltages. The complex voltage at bus k can be expressed in polar form, $v_k = |v_k|e^{\mathbf{j}\theta_k}$, where $|v_k|$ and θ_k denote the voltage magnitude and phase angle at bus k, respectively. For convenience, we also define $\theta_{k\ell} = \theta_k - \theta_\ell$ to be the angle difference across line $\{k, \ell\}$.

The $P-\Theta$ power flow problem assumes that all buses except the slack bus are PV buses. This means that the voltage magnitudes $V = (|v_1|, \ldots, |v_n|)^T$ are fixed at all buses, and the net real power injections are fixed at all buses except the slack bus. We denote the specified real power injection vector as $P = (p_2, \ldots, p_n)^T$. The unknown variable is $\Theta = (\theta_2, \ldots, \theta_n)^T$ because bus 1 is the reference bus and θ_1 is fixed at zero. Although the voltage magnitudes are considered fixed at all buses, we make no assumption about their particular values. For example, the magnitude could be low as in the two-bus example mentioned in Section I. Finally, assuming that the shunt elements of the model have zero real part, we can neglect the admittance of the shunt elements without loss of generality. That is, we assume that the shunt elements are purely reactive.

Let $i \in \mathbb{C}^n$ be the vector of complex currents, where i_k is the total current flowing out of bus k into the rest of the network. Given a complex admittance matrix $Y \in \mathbb{C}^{n\times n}$, the equation $i = Yv$ holds due to Ohm's law and Kirchoff's Current Law. Furthermore, the complex power injected at bus k is equal to $s_k = p_k + \mathbf{j}q_k = v_k i_k^H$ where p_k and q_k denote the net real and reactive power injections at bus k, respectively. Therefore, we can write the equation for the real power injections as: $p_k = \Re\{(Yv)_k^H v_k\}$. Since voltage magnitudes are known parameters, the injection vector P is only a function of Θ and we can define the following injection operator that describes the $P-\Theta$ problem.

Definition 1. *Define $\hat{P}_k : \mathbb{R}^{n-1} \to \mathbb{R}$ as the map from the vector of phasor angles to the real power injection at bus k:*

$$\hat{P}_k(\Theta) = \Re\{(Yv)_k^H v_k\}. \tag{1}$$

Moreover, define the injection operator $\hat{P} : \mathbb{R}^{n-1} \to \mathbb{R}^{n-1}$ as

$$\hat{P}(\Theta) = [\hat{P}_2(\Theta), \ldots, \hat{P}_n(\Theta)]. \tag{2}$$

The goal of the $P-\Theta$ problem is, given $P \in \mathbb{R}^{n-1}$, to find $\Theta \in \mathbb{R}^{n-1}$ such that $\hat{P}(\Theta) = P$.

IV. ACYCLIC NETWORKS

In this section, we derive conditions under which the $P-\Theta$ problem has at most one solution for a power system represented by an acyclic graph. In particular, a straightforward generalization of the elementary angle assumption that is necessary for a single line network to have at most one solution is sufficient for any acyclic network to have at most one solution.

A. Single line properties

We begin the analysis with a single line. Consider any line $\{k, \ell\} \in \mathbb{E}$ and the real power flow from bus k to bus ℓ, denoted by $p_{k\ell}$. Elementary calculations show that:

$$p_{k\ell} = G_{k\ell}(|v_k|^2 - |v_k| \cdot |v_\ell| \cos\theta_{k\ell}) + B_{k\ell}|v_k| \cdot |v_\ell| \sin\theta_{k\ell} \quad (3)$$

Therefore, given the line properties and the voltage magnitude at both ends, the flow $p_{k\ell}$ depends only on the voltage angle difference $\theta_{k\ell}$. Hereby, we define the function $\hat{p}_{k\ell}(\cdot)$ for every $\{k, \ell\} \in \mathbb{E}$ such that $p_{k\ell} = \hat{p}_{k\ell}(\theta_{k\ell})$. Taking the derivative

$$\frac{\partial \hat{p}_{k\ell}}{\partial \theta_{k\ell}}(\theta_{k\ell}) = G_{k\ell}|v_k| \cdot |v_\ell| \cdot \sin\theta_{k\ell} + B_{k\ell}|v_k| \cdot |v_\ell| \cdot \cos\theta_{k\ell}$$

concludes that $p_{k\ell}$ is monotonically increasing in $\theta_{k\ell}$ if:

$$G_{k\ell}|v_k| \cdot |v_\ell| \cdot \sin\theta_{k\ell} + B_{k\ell}|v_k| \cdot |v_\ell| \cdot \cos\theta_{k\ell} \geq 0.$$

A strict inequality of the above equation is obtained if:

$$-\tan^{-1}(B_{k\ell}/G_{k\ell}) < \theta_{k\ell} < \pi - \tan^{-1}(B_{k\ell}/G_{k\ell}).$$

Similarly, $p_{\ell k}$ is strictly monotonically decreasing in $\theta_{k\ell}$ if:

$$\tan^{-1}(B_{k\ell}/G_{k\ell}) - \pi < \theta_{k\ell} < \tan^{-1}(B_{k\ell}/G_{k\ell}).$$

Combining these observations, both $p_{k\ell}$ and $p_{\ell k}$ are strictly monotonic functions of $\theta_{k\ell}$ as long as:

$$|\theta_{k\ell}| < \tan^{-1}(B_{k\ell}/G_{k\ell}), \quad (4)$$

which corresponds to the region of steady-state stability of the line $\{k, \ell\}$ considered individually. We refer to $\tan^{-1}(B_{k\ell}/G_{k\ell})$ as the steady-state stability limit for line $e = \{k, \ell\} \in \mathbb{E}$ and will restrict attention to angles that satisfy (4) for each line $\{k, \ell\}$ in the system. In what follows, we will give the definitions on the *set of allowable angles* and *set of allowable injections*.

Definition 2. *For a power system $\mathbb{G} = (\mathbb{V}, \mathbb{E})$, let $\mathbb{G} = (\mathbb{V}, \mathbb{E}, \mathbb{W})$ indicate a weighted version of the power system network. For each line $e = \{k, \ell\} \in \mathbb{E}$, there is a corresponding angle limit (weight) $w_{k\ell} \in \mathbb{W}$ such that $\omega_{k\ell} < \tan^{-1}(B_{k\ell}/G_{k\ell})$. Note that $\omega_{k\ell}$ can be written in an equivalent notation, ω_e. The set $\mathbb{W}$ is called the 'set of allowable limits.' The 'set of allowable angles' for a power system $\mathbb{G} = (\mathbb{V}, \mathbb{E}, \mathbb{W})$ is defined as:*

$$\Gamma(\mathbb{G}) = \{\Theta \in \mathbb{R}^{n-1} : \theta_1 = 0 \text{ and } |\theta_{k\ell}| < \omega_{k\ell} \ \forall \{k, \ell\} \in \mathbb{E}\}.$$

Furthermore, for a given $\Theta \in \Gamma(\mathbb{G})$, define $\mathcal{P}(\mathbb{G}, \Theta) \in \mathbb{R}^{n-1}$ to be the vector of net injections (at all buses except for the slack bus) realized by Θ. We define $\mathcal{P}(\mathbb{G}, \Gamma(\mathbb{G})) \subseteq \mathbb{R}^{n-1}$ to be the set of all possible net injections for allowable angles and refer to it as the "set of allowable injections."

We acknowledge that there is no one-to-one correspondence between the notion of stability of a line considered individually in isolation and the *steady-state and transient stability* of an actual power system, particularly where there are additional control feedback loops such as "power system stabilizers." However, limiting angles to satisfy (4) results in some convenient properties of power flow solutions. These properties are explained in the following lemma:

Lemma 1. *Define $\underline{p}_{k\ell} = \hat{p}_{k\ell}(-\omega_{k\ell})$ and $\overline{p}_{k\ell} = \hat{p}_{k\ell}(\omega_{k\ell})$. Then for each $p_{k\ell} \in (\underline{p}_{k\ell}, \overline{p}_{k\ell})$ there exists a unique $\theta_{k\ell}$ with $|\theta_{k\ell}| < \omega_{k\ell}$ such that $p_{k\ell} = \hat{p}_{k\ell}(\theta_{k\ell})$. In fact, there is an explicit expression for the solution $\theta_{k\ell}$:*

$$\theta_{k\ell} = \hat{\theta}_{k\ell}(p_{k\ell}) = sin^{-1}\left(\frac{p_{k\ell} - G_{k\ell}|v_k|^2}{|v_k| \cdot |v_\ell| Z_{k\ell}}\right) - \gamma_{k\ell} \quad (5)$$

where $Z_{k\ell} = \sqrt{G_{k\ell}^2 + B_{k\ell}^2}$ and $\gamma_{k\ell} = \tan^{-1}(-G_{k\ell}/B_{k\ell})$. Furthermore, if we define $\hat{r}_{k\ell}(\cdot) = \hat{p}_{\ell k}(-\hat{\theta}_{k\ell}(\cdot))$, then

$$p_{\ell k} = \hat{r}_{k\ell}(p_{k\ell}) \quad (6)$$

where $\hat{r}_{k\ell}$ is a strictly decreasing function.

Previously, we established that $\hat{p}_{k\ell}(\cdot)$ is a strictly increasing function of $\theta_{k\ell}$ over the range $|\theta_{k\ell}| < \omega_{k\ell}$. By using the Browder–Minty theorem in its proof, Lemma 1 states that the inverse of the function $\hat{p}_{k\ell}(\cdot)$ is well-defined. In fact, the inverse function $\hat{\theta}_{k\ell}(\cdot)$ is also an increasing function, of $p_{k\ell}$ over $(\underline{p}_{k\ell}, \overline{p}_{k\ell})$. Moreover, given $p_{k\ell} \in (\underline{p}_{k\ell}, \overline{p}_{k\ell})$, there is a uniquely determined corresponding value for the flow $p_{\ell k}$ coming from the opposite direction. This enables us to express $p_{\ell k}$ as a well-defined function of $p_{k\ell}$ as in (6).

B. Tree networks

In this subsection, we build on the results for a single line to prove uniqueness of the $P - \Theta$ power flow problem for tree networks. We also show that the *set of allowable injections* is a convex set. Although a tree network is not realistic for transmission systems, this will provide important results that will be used for the general case of a mesh. Some of the results that we mention here are already well known in the existing literature. However, we organize the proof of this existing result around the monotonicity property, with the goal of generalizing the arguments to mesh networks.

We will write $\mathbb{T} \subseteq \mathbb{V} \times \mathbb{V}$ for a collection of lines that form a tree and consider power systems with graphs $\mathbb{G} = (\mathbb{V}, \mathbb{T}, \mathbb{W})$. Recall that the reference/slack bus is indexed by 1. A key observation about tree topology is that for any bus $k \in \mathbb{V}$ there is a unique path $E_k \subseteq \mathbb{T}$ of successive lines between bus k and bus 1, which we consider to be the root of the tree. Define the "distance" $c(k)$ between bus k and bus 1 to be the number of lines in the unique path E_k between bus k and bus 1 in $\mathbb{T}$. We define $E_1 = \emptyset$ and $c(1) = 0$. Generically, results for such networks could be proved by beginning with leaves and proceeding towards bus 1 by using an induction argument on the decreasing distance to bus 1. By following such approach, the next theorem can be obtained.

Theorem 2. *Suppose that the power system $\mathbb{G} = (\mathbb{V}, \mathbb{T}, \mathbb{W})$ has a tree topology. Then,*

1) *For each $P \in \mathcal{P}(\mathbb{G}, \Gamma(\mathbb{G}))$, there is a unique $\Theta \in \Gamma(\mathbb{G})$ such that $P = \hat{P}(\Theta)$.*
2) *$\mathcal{P}(\mathbb{G}, \Gamma(\mathbb{G}))$ is a convex set.*

Note that by Part 1 of Theorem 2, for a given power system $\mathbb{G}$ with a tree topology, there is a well-defined function $\hat{\Theta}$ such that for each $P \in \mathcal{P}(\mathbb{G}, \Gamma(\mathbb{G}))$, the unique value $\Theta \in \Gamma(\mathbb{G})$ with the property $P = \hat{P}(\Theta)$ satisfies $\Theta = \hat{\Theta}(P)$. That is, $\hat{\Theta}(\bullet)$ is the inverse of $\hat{P}(\Theta)$.

V. Cyclic Networks

For networks with cycles, restricting the voltage angles to the *set of allowable angles* is not enough to guarantee that the $P-\Theta$ problem has at most one solution. Hence, we begin this section by analyzing a simple example on a cycle to illustrate the need for additional conditions on voltage angles in guaranteeing a unique solution.

In Fig. 1, we have a six-bus lossless network where all the real power injections are set to be zero. Under this setting, we can see that there are at least two solutions: one with zero flow in all lines and another one with a nonzero flow around the cycle, corresponding to a $\pi/3$ angle difference across each line. This example is similar to the one in [7] and is essentially due to the fact that the sum of angle differences from bus 1 to bus 6 (i.e. $\theta_{12}+\theta_{23}+\theta_{34}+\theta_{45}+\theta_{56}$) is less than $-\pi$ and therefore becomes equivalent to $\pi/3 \pmod{2\pi}$, allowing a positive amount of power to flow from bus 1 to bus 6 and then back to bus 1. In this example, if the absolute value of $\theta_{12}+\theta_{23}+\theta_{34}+\theta_{45}+\theta_{56}$ were to be restricted below π, there would be no possibility of multiple solutions. We state this formally in the following lemma.

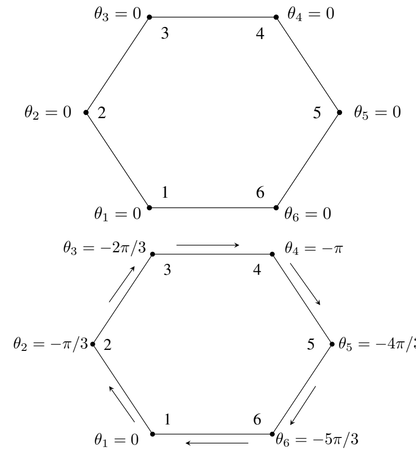

Fig. 1: Cycle example showing multiple solutions. The two graphs show two different solutions that satisfy the power flow equations. In the top solution, there is no flow going around the cycle. In the bottom solution, there is a clockwise flow going around the cycle.

Lemma 3. *Consider a power network $\mathbb{G}=(\mathbb{V},\mathbb{E},\mathbb{W})$ with $\mathbb{V}=\{1,\dots,N\}$ and $\mathbb{E}=\{\{1,2\},\dots,\{N-1,N\},\{N,1\}\}$. For every $P\in\mathcal{P}(\mathbb{G},\Gamma(\mathbb{G}))$ there is a unique solution $\Theta\in\Gamma(\mathbb{G})$ such that $P=\hat{P}(\Theta)$ if:*

$$\omega_{12}+\omega_{23}+\cdots+\omega_{N-1,N}<\pi/2. \tag{7}$$

Lemma 3 applies to only a single cycle network. However, this will be extended to any arbitrary network below. The main idea behind the development of this result is to associate a digraph to every possible distinct solution based on its deviation from a baseline solution. We call two solutions distinct if every two corresponding elements of these solutions are different. If an angle constraint similar to equation (7) is met for every such digraph (named the residual-digraph), then there cannot be multiple distinct power flow solutions (i.e., distinctly unique). In this section, we prove results on distinct uniqueness, but the same methodology can also be readily used to prove results on uniqueness (in the common sense) by substituting the digraph with a hybrid graph that contains both directed and undirected edges. In addition, if there are two non-distinct solutions, then one can delete the edges with the same flows in the two solutions and then compensate for the nodal injections at the endpoints of all such removed edges in order to arrive at a subgraph that has two distinct solutions. In other words, having only unique distinct solutions for the subgraphs of the network implies the uniqueness of the solution for the original network. As a result, we only focus on studying distinct solutions in this section. For the rest of this paper, we also assume that the digraphs under consideration do not have self-loops. Furthermore, in order to satisfy the power balance equations, there must be at least one incoming and one outgoing edge at each non-slack bus of the residual-digraph. This merits introducing the concept of *feasible orientation*, which we define below.

Definition 3. *(Feasible Orientation) Consider a general power network $\mathbb{G}=(\mathbb{V},\mathbb{E},\mathbb{W})$. Let $\mathbb{D}=(\mathbb{V},\widetilde{\mathbb{E}},\mathbb{W})$ be a digraph that is created by assigning a specific orientation $\widetilde{\mathbb{E}}$ to the original undirected edges $\mathbb{E}$ of graph $\mathbb{G}$. The digraph $\mathbb{D}$ is called a 'feasible orientation' of the underlying undirected graph if:*

$$d^+(k)\geq 1,\ d^-(k)\geq 1 \quad \forall k\in\mathbb{V}\setminus\{1\}$$

The set of all feasible orientations for graph $\mathbb{G}$ is called the 'set of feasible orientations' and is denoted by $\mathcal{D}_f(\mathbb{G})$.

The condition in Definition 3 simply requires that each bus have in-degree and out-degree greater than or equal to one. Now, we are ready to state the theorem that generalizes Lemma 3. From here on, we will use the word 'vertex' more often in place of the word 'bus.'

Theorem 4. *Consider an arbitrary power network $\mathbb{G}=(\mathbb{V},\mathbb{E},\mathbb{W})$. Suppose that for every feasible orientation $\mathbb{D}\in\mathcal{D}_f(\mathbb{G})$, there exists a directed cycle $\mathbb{C}$ with its vertex set denoted as $\mathbb{V}_{dc}=\{u(1),\dots,u(|\mathbb{V}_{dc}|)\}\subseteq\mathbb{V}$ such that*

$$\sum_{i=1}^{|\mathbb{V}_{dc}|-1}\omega_{u(i),u(i+1)}<\pi/2. \tag{8}$$

Then, for each $P\in\mathcal{P}(\mathbb{G},\Gamma(\mathbb{G}))$ there cannot be multiple distinct solutions satisfying $P=\hat{P}(\Theta)$.

Note that condition (8) becomes less restrictive if there exists a short directed cycle for every *feasible orientation* of the underlying graph. In the graph theory literature, the length of the smallest directed cycle of digraph $\mathbb{D}$ is called the *girth* of $\mathbb{D}$, which we denote by $\delta(\mathbb{D})$. Therefore, to rephrase the earlier statement, having a small *girth* for all of the possible *feasible orientations* is crucial. This calls for a new notion of *maximal girth* of an undirected graph, in addition to the *girth*, which we define below.

Definition 4. *For a given undirected graph $\mathbb{G}$, define the 'maximal girth' $\Delta(\mathbb{G})$ as follows:*

$$\Delta(\mathbb{G})=\max_{\mathbb{D}\in\mathcal{D}_f(\mathbb{G})}\delta(\mathbb{D}) \tag{9}$$

Corollary 5. *Given an arbitrary power network* $\mathbb{G} = (\mathbb{V}, \mathbb{E}, \mathbb{W})$*, suppose that*

$$\omega_{k\ell} < \frac{\pi}{2 \cdot (\Delta(\mathbb{G}) - 1)} \quad \forall \{k, \ell\} \in \mathbb{E}. \tag{10}$$

Then, for each $P \in \mathcal{P}(\mathbb{G}, \Gamma(\mathbb{G}))$ *there cannot be multiple distinct solutions satisfying* $P = \hat{P}(\Theta)$.

Note that for cyclic networks, $\mathcal{P}(\mathbb{G}, \Gamma(\mathbb{G}))$ is in general a nonconvex set, and there have been recent works that address the issue via convex restrictions [24]. So far, we have shown that finding a directed cycle satisfying condition (8) for all feasible orientations corresponds to certifying that the $P - \Theta$ problem cannot have multiple distinct solutions. Furthermore, Corollary 5 has introduced the concept of *maximal girth* to show that if the *allowable limits* are uniformly less than the upper-bound in (10), then the $P - \Theta$ problem cannot have multiple distinct solutions. The smaller the value of $\Delta(\mathbb{G})$, the more freedom there is for angle differences over lines. The question arises as to whether we can calculate or upper-bound $\Delta(\mathbb{G})$. For the example in Fig. 1, it is relatively easy to see that $\Delta(\mathbb{G}) = 6$. However, for a graph with m edges, the number of *feasible orientations* is on the order of 2^m, and calculating or even proving an upper-bound on $\Delta(\mathbb{G})$ is a difficult task. Most of the existing results provide bounds that are on the order of n/s where s is the minimum out-degree of a digraph [25], which is not useful for our purpose since $s = 1$ for *feasible orientations*.

Here, we upper-bound the *maximal girth* by using another property of the underlying undirected graph, namely the length of its longest chordless cycle, which we denoted by $\kappa(\mathbb{G})$. The basic idea behind the proof is that any directed cycle with a chord can be further decomposed into two cycles, one of which is again a directed cycle. The formal statement with its proof is provided in Lemma 10 of the Appendix. With this upper-bound on *maximal girth*, condition (10) can be substituted by the following new condition:

$$\omega_{k\ell} < \frac{\pi}{2 \cdot (\kappa(\mathbb{G}) - 1)} \quad \forall \{k, \ell\} \in \mathbb{E} \tag{11}$$

A major benefit of this result comes from the fact that $\kappa(\mathbb{G})$ can be computed in a relatively straightforward fashion. For the example in Fig. 1, the value of $\kappa(\mathbb{G})$ is equal to the value of $\Delta(\mathbb{G})$. The procedure for the computation of $\kappa(\mathbb{G})$ and its values for several IEEE test cases are reported in Section VIII-B. For complete graphs, $\kappa(\mathbb{G}) = 3$ because all vertices are connected by an edge. In connection with Corollary 5, this implies that complete graphs cannot have multiple distinct solutions if angle differences are restricted below $\pi/4$, which is often the case in real-world power operations due to security considerations. It is acknowledged, however, that power system graphs are not in practice complete graphs and are, in fact, sparse.

VI. Series-Parallel Reduction

This section shows that under the assumption that voltage angles lie within the *allowable limits*, the uniqueness of $P-\Theta$ problem solutions is preserved under *series-parallel reduction*, with appropriate updates on the *set of allowable limits*, namely $\mathbb{W}$. These updates are involved with the *dangling vertex*, *highway-path* and *parallel edges* of the graph, which will be explained in detail throughout the section. We conclude the section with a recognition that all graphs that are reducible (via series-parallel reduction) to a K_2 have a unique power flow solution if the updated *allowable limit* on the remaining single line is less than $\pi/2$. These graphs turn out to be equivalent to a group of graphs called *Generalized Series-Parallel (GSP)* that includes any tree or cycle graph. In fact, every outer-planar graph is *GSP* [26]. This result has practical implications because real-world transmission and distribution systems are not far away from this type of topology. We begin by defining *series-parallel reduction* and *GSP* graphs. As detailed in [26], one of the equivalent definitions of a *GSP* graph is as follows:

Definition 5. *A graph is a Generalized Series-Parallel (GSP) graph if it can be reduced to a single edge graph (K_2) by a sequence of the following three operations:*

1. *Replacement of a pair of parallel edges with a single edge that connects their common endpoints.*
2. *Replacement of a pair of edges incident to a vertex of degree 2 with a single edge.*
3. *Deletion of a dangling (degree 1) vertex.*

Any sequence of these three operations will be called a "series-parallel reduction".

To help visualize how the three operations work, in Fig. 2, we illustrate a reduction example on the IEEE 14-bus network. Starting from the original network (a), the graph is subsequently reduced to (d) via a sequence of series-parallel reductions. Going from (a) to (b) represents an example of operation 3, where the dangling vertex (numbered by 8 in the figure) is deleted. The process from (b) to (c) is an example of operation 2, where two edges incident to a vertex of degree 2 is replaced by a single edge. Finally, the process from (c) to (d) is an example of operation 1, where two parallel edges are replaced by a single edge.

It turns out that the analysis of conditions (8–11) for the original power network can be performed on a "series-parallel reduced" network that could be far smaller than the original graph. Let us revisit the example in Fig. 2. In the original network (a), edge $\{7, 8\}$ cannot be part of any cycle because vertex 8 has degree 1. Therefore, this edge can be omitted from the analysis of directed cycles. In network (b), edges $\{6, 12\}$ and $\{12, 13\}$ have to be either both part of a cycle or both not part of any cycle. Therefore, the two edges can be replaced by a single edge $\{6, 13\}$ with a new *allowable limit*, $\widetilde{\omega}_{6,13} = \omega_{6,12} + \omega_{12,13}$. A similar implication follows if we replace the two parallel edge in (c), connecting vertex 6 and 13, by a single edge with a new *allowable limit* that is of maximum value among the replaced edges. Before we present the formal statement of this observation, we define what a *highway-path* is below.

Definition 6. *An induced path* $\mathbb{P}$ *of* $\mathbb{G}$ *with vertex set*

$$\mathbb{V}^h = \{s, u^h(1), u^h(2), \ldots, u^h(H), t\} \tag{12}$$

from vertex s *to vertex* t *is called a highway-path if:*

$$d(u^h(i)) = 2 \quad \forall i \in \{1, \ldots, H\} \tag{13}$$

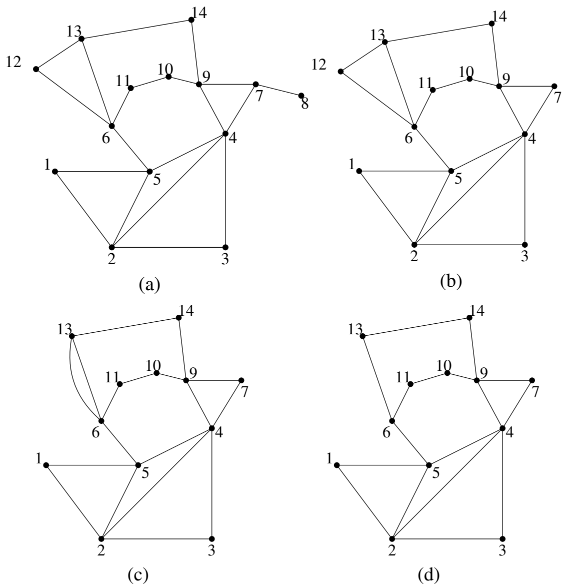

Fig. 2: A simple diagram illustrating a sequence of series-parallel reductions for the IEEE 14-bus system.

and $u^h(i)$ is a non-slack vertex for every $i \in \{1, \ldots, H\}$.

Note that a single edge is also considered a *highway-path*. By building on the previous observations and using the above definition, we show that the problem of determining the uniqueness of the power flow solutions for the original meshed network can be reduced to determining the uniqueness of solutions on a smaller graph that excludes a *dangling vertex*, a *highway-path* or a *parallel edge*.

Theorem 6. *Consider a power network $\mathbb{G} = (\mathbb{V}, \mathbb{E}, \mathbb{W})$.*
1. If $\mathbb{G}$ contains two parallel edges $e_1, e_2 \in \mathbb{E}$ both connecting the same pair of vertices, define

$$\bar{\mathbb{V}} = \mathbb{V},\ \bar{\mathbb{E}} = \mathbb{E} \setminus \{e_2\},$$

$$\bar{\mathbb{W}} = \{\bar{w}_e \mid \bar{w}_e = w_e,\ \forall e \in \bar{\mathbb{E}} \setminus \{e_1\},\ \bar{\omega}_{e_1} = \max\{w_{e_1}, w_{e_2}\}\}$$

2. If $\mathbb{G}$ contains a highway-path $\mathbb{P}$, let $\mathbb{V}^h$ be the vertex set of $\mathbb{P}$ as described in (12). Define

$$\bar{\mathbb{V}} = \mathbb{V} \setminus \{u^h(1), \ldots, u^h(H)\},\ \bar{\mathbb{E}} = \mathbb{E}[\bar{\mathbb{V}}] \cup \{\{s, t\}\},$$

$$\bar{\mathbb{W}} = \{\bar{w}_e \mid \bar{w}_e = w_e,\ \forall e \in \mathbb{E}[\bar{\mathbb{V}}],\ \bar{\omega}_{s,t} = \sum_{e \in \mathbb{E}[\mathbb{V}^h]} \omega_e\}$$

3. If $\mathbb{G}$ contains a dangling (degree 1) vertex u, define

$$\bar{\mathbb{V}} = \mathbb{V} \setminus \{u\},\ \bar{\mathbb{E}} = \mathbb{E}[\bar{\mathbb{V}}],\ \bar{\mathbb{W}} = \{\bar{w}_e \mid \bar{w}_e = w_e,\ \forall e \in \bar{\mathbb{E}}\}$$

Let the reduced graph G^r be defined by $\mathbb{G}^r = (\bar{\mathbb{V}}, \bar{\mathbb{E}}, \bar{\mathbb{W}})$. Then, the $P - \Theta$ power flow problem for the original graph $\mathbb{G}$ has at most one solution if condition (10) is satisfied for $\mathbb{G}^r$.

Theorem 6 implies that deleting the graph's *dangling vertex*, or contracting multiple edges that are connected in series, or eliminating one of the two parallel edges do not influence the uniqueness of power flow solutions as long as the *set of allowable limits* $\mathbb{W}$ is updated appropriately. One major advantage of Theorem 6 is that the analyses pertaining to *directed cycles*, *maximal girth* and *longest chordless cycle* introduced in Section V can now be applied to a smaller reduced network. For instance, checking condition (8) is time-dependent on the number of vertices, edges, and simple cycles of a graph. As the graph becomes larger, this computation can be daunting since the number of simple cycles can grow exponentially in the number of vertices. The effect of series-parallel reduction on several IEEE test cases is illustrated in Section VIII-A.

Finally, it is no coincidence that these three reduction procedures are equivalent to the three operations that are allowed and required to turn a *GSP* graph into a K_2 graph (see Definition 5). In other words, any *GSP* graph can be reduced to a single line after undergoing a sequence of reduction procedures delineated in Theorem 6. The absence of cycles suggests that Theorem 4 is unnecessary in this case, and warrants a simpler result, which is given as a corollary below. The corollary states that the $P - \Theta$ problem on *GSP* graphs has at most one solution if the final updated *allowable limit* for the reduced single line is less than $\pi/2$.

Corollary 7. *Suppose that the power system $\mathbb{G} = (\mathbb{V}, \mathbb{E}, \mathbb{W})$ has a GSP topology. Let $\mathbb{L} = (\bar{\mathbb{V}}, \bar{\mathbb{E}}, \bar{\mathbb{W}})$ be a K_2 graph (containing the slack bus) that is series-parallel reduced from $\mathbb{G}$, where $\bar{\mathbb{W}} = \{\omega\}$ represents the 'allowable limit' on the remaining line that is updated according to the procedures in Theorem 6. If $\omega < \pi/2$, then there is a unique $\Theta \in \Gamma(\mathbb{G})$ such that $P = \hat{P}(\Theta)$ for each $P \in \mathcal{P}(\mathbb{G}, \Gamma(\mathbb{G}))$.*

VII. Algorithm

In this section, we design an algorithm for finding the unique solution of the $P - \Theta$ problem when the graph has a *GSP* structure. In general, the $P - \Theta$ equations constitute a system of nonlinear equations and are prone to complex and chaotic behavior. Conventional algorithms such as Newton's method may fail to converge when a bad initial guess is provided or if the system is close the its security margins. In the special case where the injection operator $\hat{P}(\Theta)$ is strictly monotone, leading to a unique (if there exists) $P - \Theta$ problem solution, a fixed point iteration approach will converge to the correct solution with a convergence rate that depends on the monotonicity constant and Lipschitz constant of the operator in question. However, requiring the injection operator to be monotonic over a feasible region is quite restrictive. In our case, the uniqueness of the $P - \Theta$ power flow problem for *GSP* graphs emerges from a repetitive reduction process of the network and its flow set in a parameterized way that is not amenable to conventional numerical methods. The power flow algorithm that we propose for the *GSP* networks, therefore, will emulate this reduction process.

A. Linear-time algorithm

We begin with a simple example illustrating the idea behind the algorithm. Fig. 3 shows a *GSP* network with four buses and five lines, where bus 1 is the slack bus as usual. Let $\mathbb{W} = \{\omega_{1,2},\ \omega_{2,3},\ \omega_{1,3},\ \omega_{1,4},\ \omega_{3,4}\}$ denote the *set of allowable limits* for this network. Suppose that the assumption in Corollary 7 is met, meaning that the network can be reduced to a single edge connecting vertices 1 and 4 via series-parallel reduction and the updated *allowable limit* for that edge is less than $\pi/2$. More specifically, this means that $\bar{\omega}_{1,4} < \pi/2$, where $\bar{\omega}_{1,4}$ equals the left-hand side of the following expression:

$$\max\Big\{\omega_{1,4}\ ,\ \max\{\omega_{1,2}+\omega_{2,3}\ ,\ \omega_{1,3}\}+\omega_{3,4}\Big\} < \pi/2 \quad (14)$$

Now, set the variable x to represent the real power flow from vertex 1 to vertex 2, i.e. $x = p_{12}$. Due to power balance at each vertex and the fact that vertex 2 has a degree of two, p_{23} is an increasing function with respect to x. Furthermore, due to Lemma 1 and the allowable angle assumptions that we made, this means that θ_{12} and θ_{23} are also increasing functions of p_{12}. It follows that $\theta_{13} = \theta_{12} + \theta_{23}$ is also an increasing function of x. Finally, due to the assumption on $\bar{\omega}_{1,4}$ in (14), we know that $\omega_{1,3} < \frac{\pi}{2}$, which implies that p_{13} is an increasing function of θ_{13} and also of x.

Similarly, the flow variables expressed as bold arrows in Fig. 3 are all monotonically increasing with respect to x. Furthermore, once x is known, all the other flow variables can be calculated sequentially. We will call this flow variable x the *primary flow*. This sequential process is illustrated below:

1. Set $\mathbf{x} = x^0$.
2. Calculate: $\mathbf{p_{23}} = p_2 - \hat{r}_{12}(x)$
3. Calculate θ_{12} and θ_{23}. Then, add them up to obtain θ_{13}.
4. Calculate $\mathbf{p_{13}} = \hat{p}_{13}(\theta_{13})$.
5. Calculate: $\mathbf{p_{34}} = p_3 - \hat{r}_{23}(p_{23}) - \hat{r}_{13}(p_{13})$.
6. Calculate: $\mathbf{p_{41}} = p_4 - \hat{r}_{34}(p_{34})$.

These steps will be embedded in the algorithm proposed in this section. Each iteration of the algorithm will involve the above calculation of the flow variables, followed by an update on the value of the *primary flow*. Notice that at each step of the process, all the necessary information is already calculated in the preceding steps. Also, none of the steps involves solving a separate optimization problem and just requires simple algebraic calculations. Before delving into the full algorithm, we introduce a concept of *outer-cycles*.

Definition 7. *An induced cycle $\mathbb{C}$ of $\mathbb{G}$ is called an outer-cycle if the following two conditions are met:*

1. *$\mathbb{C}$ contains two highway-paths such that the union of the two paths is $\mathbb{C}$ and the intersection is $\{s,t\}$. One of the paths (arbitrarily chosen), denoted by $\mathbb{S}^p$, will be called the principal-path and has vertex set $\mathbb{V}^p$. The other path, named $\mathbb{S}^a$, will be called the auxiliary-path and has vertex set $\mathbb{V}^a$. Let the vertex sets be denoted as follows:*

$$\mathbb{V}^p = \{s, u^p(1), u^p(2), \ldots, u^p(N), t\} \quad (15)$$
$$\mathbb{V}^a = \{s, u^a(1), u^a(2), \ldots, u^a(M), t\} \quad (16)$$

2. *All the vertices except for s and t have degree 2 and are non-slack buses.*

The concept of an *outer-cycle* is useful because it corresponds to a cycle that is reduced via a combination of operations 1 and 2 of the series-parallel reduction (Definition 5). For example, in Fig. 2, the outer-cycle with vertices $\{6, 12, 13\}$ is reduced as it is transformed from sub-figure (b) to (d). The order in which outer-cycles and dangling vertices are deleted essentially define the series-parallel reduction. In our algorithm, it also corresponds to the order in which the flows are calculated starting from the *primary flow*. Theorem 8 states that for a subset of *GSP* graphs, the exemplary steps above can work and the $P-\Theta$ power flow problem can be solved in linear time. Here, we will use the notation $\mathbb{G} \to \mathbb{G}^r$ to signify the series-parallel reduction from graph $\mathbb{G}$ to $\mathbb{G}^r$.

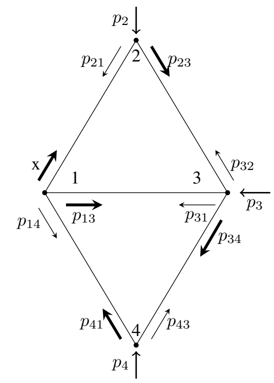

Fig. 3: A two-cycle network sharing an edge

Theorem 8. *For Corollary 7, suppose that $\mathcal{O} = \{\mathbb{C}_1, \ldots, \mathbb{C}_R\}$ is the sequence of outer-cycles reduced in the process $\mathbb{G} \to \mathbb{L}$. Let $\mathbb{E}_j$ denote the edge set for cycle $\mathbb{C}_j$. Then, there is a linear-time algorithm with complexity $O(|\mathbb{E}|\cdot log(1/\epsilon))$ to find the unique solution of the $P-\Theta$ power flow problem, given a desired precision level ϵ, if the following condition holds:*

$$|\ (\bigcup_{i<j} \mathbb{E}_i) \cap \mathbb{E}_j\ | \leq 1 \quad \forall j = \{1, \ldots, R\} \quad (17)$$

The linear-time algorithm is given in Algorithm 1. The algorithm makes use of the fact that for each line, there is one direction for which the flow increases with respect to the *primary flow* and another for which the flow decreases with respect to the *primary flow*. Let $\mathcal{F}^+$ denote the set of ordered pair of indices (k,ℓ) such that $p_{k\ell}$ is monotonically increasing with respect to the *primary flow*. Also, for notation reasons, let $p(k,\ell)$ also denote the flow from bus k to ℓ in addition to $p_{k\ell}$. Below, we define a type of projection operator Π that allows the iterative sequence to stay in the *allowable sets* arising from our angle difference assumptions. Here, x^{iter} denotes the iter$^{\text{th}}$ iteration value of the *primary flow* x. Furthermore, we make use of several MATLAB functions: *break* means to break out of all the for-loops, and *find*$(A == a)$ returns the index of an array A for which the value is equal to a.

$$\Pi(x^{\text{iter}}, p_{k\ell}) = \begin{cases} x^{\text{iter}+1} = \frac{\underline{x}+x^{\text{iter}}}{2} \text{ and } \textbf{break} & \text{if } p_{k\ell} \geq \overline{p}_{k\ell} \\ x^{\text{iter}+1} = \frac{x^{\text{iter}}+\overline{x}}{2} \text{ and } \textbf{break} & \text{if } p_{k\ell} \leq \underline{p}_{k\ell} \\ \theta_{k\ell} = \hat{\theta}_{k\ell}(p_{k\ell}) & \text{otherwise} \end{cases}$$

Each iteration of Algorithm 1 involves calculating all the flows in the set $\mathcal{F}^+$ based on the current value of the *primary flow*. This process is done sequentially in the same order in which the original graph is reduced to the final K_2 graph. Based on these values, the *primary flow* is updated by the bisection method until the solution is found. In Section VIII-C, a set of representative numerical examples are generated and the performance of this proposed algorithm is illustrated.

Algorithm 1: Linear-time GSP algorithm

Initialize: Set $\epsilon, \delta^0 > \epsilon$, P and iter $= 0$
Delete dangling vertex k and add injection value of $-\hat{r}_{k,\ell}(p_k)$ to its unique adjacent bus ℓ: $P_\ell = P_\ell - \hat{r}_{k,\ell}(p_k)$. Do this for all dangling vertices.
Set reduction order: Find the sequence of outer-cycles that are eliminated during the sp-reduction process.

$$\Rightarrow \mathcal{O} = \{\mathbb{C}_1, \ldots, \mathbb{C}_R\}$$

For each cycle $\mathbb{C}_j \in \mathcal{O}$: set the principal ($\mathbb{S}_j^p$) and auxiliary ($\mathbb{S}_j^a$) paths of $\mathbb{C}_j$ so that $\mathbb{S}_j^p$ be the path with one edge. Order the vertices in $\mathbb{S}_j^a$ as $\mathbb{V}_j^a = \{u_j^a(1), \ldots, u_j^a(M_j)\}$ so that $(u_j^a(1), u_j^a(2)) \in \mathcal{F}^+$.
Set primary flow x to represent $p(u_1^a(1), u_1^a(2))$. Then, **do** $\overline{x} = \overline{p}(u_1^a(1), u_1^a(2))$, $\underline{x} = \underline{p}(u_1^a(1), u_1^a(2))$, $x^0 = \frac{1}{2}(\underline{x} + \overline{x})$, $u_0^a(1) = u_1^a(1)$
while $|\delta^{iter}| > \epsilon$ **do**
  for *j=1:R* **do**
    z = find($\mathbb{V}_j^a == u_{j\text{-}1}^a(1)$)
    for $f = 1 : z$-1 **do**
      $k = u_j^a(z-f), \ell = u_j^a(z-f+1)$
      $q = u_j^a(z-f+2)$
      $p(k,\ell) = \hat{r}_{k,\ell}(P_\ell - p(\ell, q))$, $\Pi(x^{\text{iter}}, p(k,\ell))$
    end
    for $f = z : M_j$-2 **do**
      $k = u_j^a(f+1), \ \ell = u_j^a(f+2), \ q = u_j^a(f)$
      $p(k,\ell) = P_k - \hat{r}_{q,k}(p(q,k))$ $\Pi(x^{\text{iter}}, p(k,\ell))$
    end
    $w_j = \sum_{k=1}^{M_j-1} \theta_{u_j^a(k), u_j^a(k+1)}$
    $p(u_j^a(1), u_j^a(M_j)) = \hat{p}_{u_j^a(1), u_j^a(M_j)}(w_j)$
    $P_{u_j^a(1)} = P_{u_j^a(1)} - p(u_j^a(1), u_j^a(2))$
    $P_{u_j^a(M_j)} = P_{u_j^a(M_j)} + p(u_j^a(M_j - 1), u_j^a(M_j))$
    Delete dangling vertex k**,** and add injection value of $-\hat{r}_{k,\ell}(p_k)$ to its unique adjacent bus ℓ: $P_\ell = P_\ell - \hat{r}_{k,\ell}(p_k)$
  end
  $p(u_R^a(M_R), u_R^a(1)) =$
  $P_{u_R^a(M_R)} - p(u_R^a(M_R - 1), u_R^a(M_R))$
  $\Pi(x^{\text{iter}}, p(u_R^a(M_R), u_R^a(1)))$
  $\delta^{\text{iter}} = w_R + \theta_{u_R^a(M_R), u_R^a(1)}$
  if $\delta^{iter} > 0$ **then**
    $\overline{x} = x^{\text{iter}}, \ x^{\text{iter}+1} = \frac{1}{2}(\overline{x} + \underline{x})$
  else
    $\underline{x} = x^{\text{iter}}, \ x^{\text{iter}+1} = \frac{1}{2}(\overline{x} + \underline{x})$
  end
  iter $=$ iter $+ 1$
end

B. Graphs that do not satisfy the assumption in Theorem 8

Theorem 8 states that if a power system network with *GSP* topology satisfies (17), then the power flow problem can be solved efficiently. Equation (17) essentially requires that any chordless cycle can only share at most one edge with all the previous reduced cycles. Obviously, this result weakens once the assumption is not met. We will illustrate the difficulties that arise using the IEEE 14-bus system, which has a *GSP* topology but does not satisfy (17).

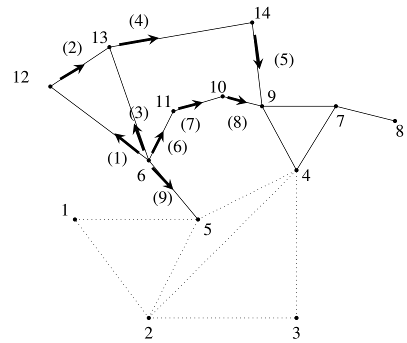

Fig. 4: A simple diagram of the IEEE 14-bus system. Buses are marked in plain numbers, while the flow variables are marked in parenthesized numbers in the order in which they are calculated in Algorithm 1. Nodal real power injections are not shown in order to simplify the diagram.

Consider the system drawn in Fig. 4 and notice that $p_{6,12}$ is selected as the *primary flow*. Given the *primary flow* value, the flows (2)–(5) can be easily calculated as delineated in Section VII-A. The first difficulty arises when trying to calculate the next unknown, flow (6). This is because the assumption of Theorem 8 breaks down: cycle $\{6, 13, 14, 9, 10, 11, 6\}$ and cycle $\{5, 6, 11, 10, 9, 4, 5\}$ share three edges. Therefore, even though we know $\theta_{6,9}$ from the previous calculations, i.e. by doing $\theta_{69} = \hat{\theta}_{6,13}(p_{6,13}) + \hat{\theta}_{13,14}(p_{13,14}) + \hat{\theta}_{14,9}(p_{14,9})$, finding flow (6) requires solving an additional implicit function. Noting that $p_{11,10} = P_{11} - \hat{r}_{6,11}(p_{6,11})$ and $p_{10,9} = P_{10} - \hat{r}_{11,10}(p_{11,10}) = P_{10} - \hat{r}_{11,10}(P_{11} - \hat{r}_{6,11}(p_{6,11}))$, the implicit function to be solved is:

$$\hat{\theta}_{6,11}(p_{6,11}) + \hat{\theta}_{11,10}(P_{11} - \hat{r}_{6,11}(p_{6,11})) \\ + \hat{\theta}_{10,9}(P_{10} - \hat{r}_{11,10}(P_{11} - \hat{r}_{6,11}(p_{6,11}))) = \theta_{6,9}$$

where the only variable is now $p_{6,11}$. This equation is monotonically increasing in $p_{6,11}$ and can be solved in $\log(1/\epsilon)$. After having found the value for flow (6), flows (7)–(9) can be found by simple arithmetic calculations. Similarly, $p_{9,7}$ can be found by solving another monotonic implicit function. This is because the nodal injection at bus 8 gives a unique $p_{7,8}$ that acts as an additional negative injection at bus 7. After this, $p_{9,4}$ and $p_{7,4}$ can be calculated by explicit arithmetic equations. The next difficulty arises after these steps. At this point, buses 5 and 4 both have three lines where the flows are unknown, which means that there is no easy way to calculate the remaining flow variables of the network. The only thing left to do is to solve a sub-problem on a subsystem of the original network, which is depicted in Fig. 4 as dotted lines. For this sub-problem, it is important to update the original nodal real power injections at bus 5, namely P_5, by $P_5 - \hat{r}_{6,5}(p_{6,5})$. Likewise, the original nodal real power injections at bus 9, namely P_9, by $P_9 - \hat{r}_{10,9}(p_{10,9}) - \hat{r}_{14,9}(p_{14,9})$. Also, update injection at bus 4 in a similar manner. Now, observe that this subsystem satisfies all the assumptions made in Theorem 8 and hence the sub-problem can be solved in linear time.

The example above illustrates the fact that violating the assumptions corresponds to an increase in the algorithm's complexity. Suppose that the original graph $\mathbb{G}$ can be divided into two subgraphs: the first part containing all the difficulties and the second part satisfying the assumptions made in Theorem 8. Then, the complexity of the algorithm will become $\mathcal{O}\Big(\{m_1 c_1 log(1/\epsilon)\} \cdot m_2 log(1/\epsilon)\Big) = \mathcal{O}\Big(c_1 m_1 m_2 log^2(1/\epsilon)\Big)$ where m_i's are the number of edges for each subgraph and c_1 is the number of additional implicit functions that have to be solved for the first subgraph.

VIII. Numerical and Simulation Results

In this section, we use simulation and computation to numerically verify and support the ideas that have been developed in the paper. We start with visualizing how series-parallel reduction works on actual power systems. Then, we calculate the longest chordless cycle – which provides an upper bound on *maximal girth* – of benchmark power systems. Finally, we apply Algorithm 1 to a class of networks in order to demonstrate its performance.

A. Series-parallel reduction of IEEE test cases

In Section VI, we introduced series-parallel reduction and showed that analyzing the uniqueness of the $P-\Theta$ problem solution can be performed on a smaller 'series-parallel reduced' network. In Fig. 5, we illustrate how these reductions visualize when applied to actual IEEE test cases (note that here the slack bus was not necessarily selected as bus 1). Figures 5(a) and (c) represent the graphs before the reduction and figures 5(b) and (d) represent the graphs after the series-parallel reduction. We can see that the reduced graphs are much smaller and contain the core information of the original graph. These reductions make Theorem 4 more practical to use because condition (8) is much easier to check on a smaller network.

B. Calculation of $\kappa(\mathbb{G})$

In Section V, we introduced $\kappa(\mathbb{G})$ as an upper-bound on the *maximal girth* $\Delta(\mathbb{G})$, which is computationally more tractable than $\Delta(\mathbb{G})$. To find the value of $\kappa(\mathbb{G})$, we first use a function built in Sage [27] to calculate all simple cycles of the graph, and then narrow them down to chordless cycles. Ultimately the length of the longest chordless cycle is obtained. The values are calculated for several IEEE standard test cases and reported in Table I. A tighter bound can be found by observing that chordless cycles are not entirely immune to further decomposition. For example, consider the IEEE 39-bus network depicted in Fig. 5(c). One of the chordless cycles that are found using our implementation is $\{1, 2, 3, 4, 14, 13, 12, 11, 6, 7, 8, 9, 39, 1\}$, which has length thirteen (note that this is not the longest chordless cycle). This is a chordless cycle because there is no edge directly connecting any two vertices of the cycle. However, as we can observe from Fig. 6, this cycle can be further partitioned into three smaller chordless cycles by the three edges in its interior. Furthermore, depending on the orientation of these three edges, at least one of the three smaller cycles is again a directed cycle if the big cycle is oriented. The tighter bound

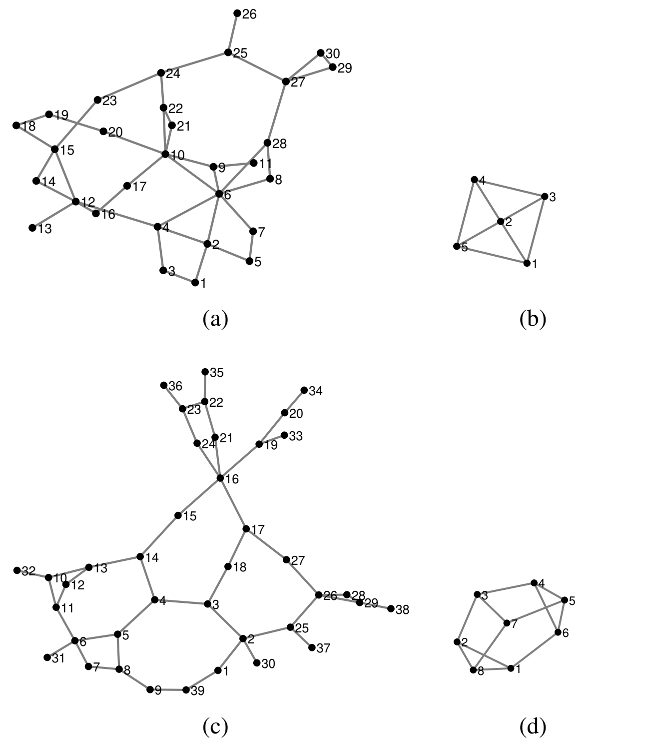

Fig. 5: (a) IEEE 30-bus system before reduction, (b) IEEE 30-bus system after reduction, (c) IEEE 39-bus system before reduction, and (d) IEEE 39-bus system after reduction.

achieved from this process is denoted by $\widetilde{\kappa}(\mathbb{G})$ and also reported in Table I. Now, Corollary 5 can be used to study when the power flow equations have a unique solution.

C. Performance of linear-time algorithm

In order to verify the effectiveness of the proposed algorithm, we analyze its performance along with the performance of Newton-Raphson method as a standard algorithm used to solve power-flow in practice. To implement this standard algorithm, we use the MATPOWER [28] *runpf* function with the 'Newton-Raphson (NR)' option. Furthermore, in order to satisfy the assumptions in equation (17), we create a class of triangulated networks of varying sizes (see Appendix J. for figure) using the MATPOWER casefile format (mpc). The *allowable set of angles* is enforced by setting the 12^{th} and 13^{th} columns of the field "branch" in the casefile to the *steady-state stability limit* (refer to Definition 2). Note that the matpower-NR algorithm cannot enforce additional angle constraints, such as (14), whereas Algorithm 1 does by design. Note that matpower-NR can be modified to incorporate these constraints if we formulate the power flow problem as an optimal power flow (OPF) problem, but then this becomes a constrained nonconvex optimization problem which introduces its own difficulties and is not the subject of this paper (even finding a feasible point to such optimization problem is a challenge). The following steps describe the experiments:

1) Generate a random Θ^* that belongs to the set $\Gamma(\mathbb{G})$. This is the true set of angles that we wish to recover via the above algorithms.

	$\kappa(\mathbb{G})$	$\widetilde{\kappa}(\mathbb{G})$
case5	4	4
case14	6	6
case30	11	8
case39	17	8

TABLE I: Upper-bounds on maximal girth for IEEE test cases.

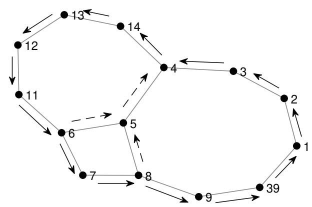

Fig. 6: Further decomposition of a directed chordless cycle. The solid arrows represent the original directed chordless cycle. The dotted arrows represent a possible orientation of the three edges that lie in the interior of the cycle.

2) Calculate the real power injection vector P, using Θ^*.
3) Taking P as input, solve the $P - \Theta$ power flow problem using both Algorithm 1 and matpower-NR method. The voltage angles retrieved from each algorithm are denoted by Θ^1 and Θ^{NR}, respectively.
4) Calculate the errors $\|\Theta^1 - \Theta^*\|_2$ and $\|\Theta^{NR} - \Theta^*\|_2$.

For the initial point that is provided to the MATPOWER solvers, we generate a random point around the true solution via $\Theta^{init} = \Theta^* + \Theta^{noise}$, where Θ^{noise} is a random vector whose elements are independent and normally distributed with mean μ. For the initialization of Algorithm 1, a random value is chosen between the minimum and maximum allowable real power flow. In order to highlight the performance of the two algorithms as the initial point deviates away from the true solution, we test three different values of $\mu = \{0.1, 1, 10\}$. The experiments are performed on an increasing number of buses and 20 independent simulations are carried out for each fixed network. Fig. 7 shows the results of these experiments. The top three figures plot the average 2-norm error (for varying values of μ) and the bottom three figures plot the average solver time (for varying values of μ) as a function of the network size. From the top three figures, it can be observed that matpower-NR performs relatively well and is able to recover Θ^* when the initial point is close enough to Θ^*. However, as Θ^{init} deviates further away from Θ^*, matpower-NR fails to reliably recover Θ^*. In fact, for most cases with initial values far from the true solution, the matpower-NR algorithm does not even converge within the maximum iteration limit. For $\mu = 10$, the matpower-NR method successfully converged for only 36 out of the 400 simulations. Fig. 8 plots the errors for these 36 convergent cases. It can be seen that several of these display high errors despite the successful convergence, implying that the algorithm converged to a different solution. Furthermore, it is demonstrated that Algorithm 1 does not converge to any of these different solutions and is capable of recovering Θ^* irrespective of the initial point or the number of buses. Finally, from the bottom three figures, we can observe that the solving time for Algorithm 1 has a very slow growth in the

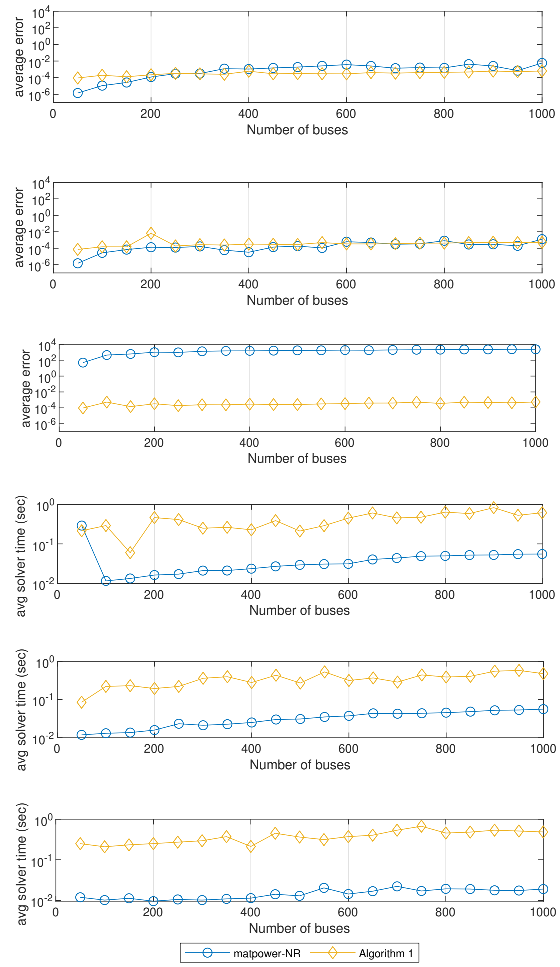

Fig. 7: Comparison of average errors and solving times for Algorithm1 and matpower-NR. The first three figures plot the average error for different values of $\mu = 0.1, 1, 10$ (from top to bottom). The last three figures plot the average solving time for different values of $\mu = 0.1, 1, 10$ (from top to bottom)

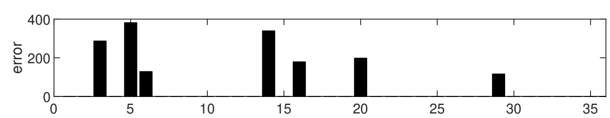

Fig. 8: Errors for the 36 (out of 400) simulations when matpower-NR converged successfully for $\mu = 10$.

size of the network and therefore can be used to solve large-scale problems. Note that Algorithm 1 was implemented in MATLAB with no strenuous efforts at optimizing the solving time and the purpose of Fig. 7 is only to demonstrate linear-time complexity of the proposed algorithm.

IX. Conclusion

In this paper, we establish sufficient conditions for the uniqueness of power flow solutions (if it exists) in an AC power system via the monotonic relationship between real power flows and voltage phase angles. We extend a simple observation made for a single line network – that angle differences bounded by their stability limit will give monotonicity and uniqueness – to the general network with multiple lines. More specifically, we prove that the $P-\Theta$ power flow problem has at most one solution for any acyclic or *GSP* graphs. These conditions guarantee the uniqueness of power flow solution, if it exists. In addition, for arbitrary power networks, we show that multiple distinct solutions cannot exist under the assumption that angle differences across the lines are bounded by some limit related to the maximal girth of the network. It is also shown that the series-parallel reduction on a graph does not alter the uniqueness of $P-\Theta$ problem solutions and therefore the analysis for a large network can be performed on a much smaller "reduced" network. Finally, we develop a efficient algorithm for a subset of the *GSP* graphs that work reliably, irrespective of the initial point.

References

[1] S. Park, R. Y. Zhang, R. Baldick, and J. Lavaei, "Monotonicity between phase angles and power flow and its implications for the uniqueness of solutions," *52nd Hawaii International Conference on System Sciences (HICSS)*, 2019.

[2] H.-D. Chiang and M. E. Baran, "On the existence and uniqueness of load flow solution for radial distribution power networks," *IEEE Transactions on Circuits and Systems*, vol. CAS-37, no. 3, pp. 410–416, March 1990.

[3] I. A. Hiskens and R. J. Davy, "Exploring the power flow solution space boundary," *IEEE Transactions on Power Systems*, vol. 16, no. 3, pp. 389–395, August 2001.

[4] H. D. Nguyen and K. S. Turitsyn, "Appearance of multiple stable load flow solutions under power flow reversal conditions," in *Proceedings of the IEEE PES General Meeting, National Harbor, MD*, July 2014, available from: https://arxiv.org/pdf/1404.6591.pdf.

[5] T. Overbye, "Lecture Notes: ECEN 460 power systems operation and control," 2017, available from: https://overbye.engr.tamu.edu/course-2/ecen460fa2017/lecture-notes/.

[6] M. Ilic, "Network theoretic conditions for existence and uniqueness of steady state solutions to electric power circuits," in *Proceedings of the IEEE International Symposium on Circuits and Systems*, 1992.

[7] A.J.Korsak, "On the question of uniqueness of stable load-flow solutions," *IEEE Transactions on Power Apparatus and Systems*, vol. PAS-91, no. 3, pp. 1093–1100, May 1972.

[8] A. Araposthatis, S. Sastry, and P. Varaiya, "Analysis of power-flow equation," *International Journal of Electrical and Power Energy Systems*, vol. 3, pp. 115–126, July 1981.

[9] F. Galiana, "Analytical investigation of the power flow equations," 1983, pp. 411–415.

[10] J. Thorp, D. Schulz, and M. Ilic-Spong, "Reactive power-voltage problem: conditions for the existence of solution and localized disturbance propagation," *International Journal of Electrical and Power Energy Systems*, vol. 9, January 1986.

[11] K. Miu and H.-D. Chiang, "Existence, uniqueness, and monotonic properties of the feasible power flow solution for radial three-phase distribution networks," *IEEE Transactions on Circuits and Systems*, vol. 47, pp. 1502–1514, October 2000.

[12] K. Dvijotham, E. Mallada, and J. Simpson-Porco, "High-voltage solution in radial power networks: existence, properties, and equivalent algorithms," *IEEE Control Systems Letters*, vol. 1, no. 2, pp. 322–327, October 2017.

[13] J. Lavaei, D. Tse, and B. Zhang, "Geometry of power flows in tree networks," *IEEE Transactions on Power Systems*, vol. 31, pp. 163–172, January 2016.

[14] T. Chen and D. Mehta, "On the network topology dependent solution count of the algebraic load flow equations," *IEEE Transactions on Power Systems*, vol. 33, no. 2, pp. 1451–1460, March 2018, available from:https://arxiv.org/pdf/1512.04987.pdf.

[15] F.F.Wu, "Theoretical study of the convergence of the fast decoupled load flow," *IEEE Transactions on Power Apparatus and Systems*, vol. PAS-96, no. 1, pp. 268–275, January 1977.

[16] C. Wang, A. Bernstein, J.-Y. Le Boudec, and M. Paolone, "Explicit conditions on existence and uniqueness of load-flow solutions in distribution networks," *IEEE Transactions on Smart Grid*, vol. 9, no. 2, pp. 953–962, March 2018.

[17] S. Z. S. Bolognani, "On the existence and linear approximation of the power flow solution in power distribution networks," *IEEE Transactions on Power Systems*, vol. 31, pp. 163–172, January 2016.

[18] J. W. Simpson-Porco, "A theory of solvability for lossless power flow equations – part I: Fixed-point power flow," *IEEE Transactions on Control of Network Systems*, vol. 5, no. 3, pp. 1361–1372, September 2018.

[19] ——, "A theory of solvability for lossless power flow equations – part II: Conditions for radial networks," *IEEE Transactions on Control of Network Systems*, vol. 5, no. 3, pp. 1373–1385, September 2018.

[20] A. Bernstein, C. Wang, E. Dall'Anese, J.-Y. L. Boudec, and C. Zhao, "Load-flow in multiphase distribution networks: Existence, uniqueness, non-singularity and linear models," *IEEE Transactions on Power Systems*, vol. 33, no. 6, pp. 5832–5843, April 2018.

[21] B. Cui and X. A. Sun, "Solvability of power flow equations through existence and uniqueness of complex fixed point," 2019, available online at https://arxiv.org/pdf/1904.08855.pdf.

[22] K. Dvijotham, S. Low, and M. Chertkov, "Solving the power flow equations: a monotone operator approach," *archived and available at https://arxiv.org/pdf/1506.08472.pdf*, 2015.

[23] S.Jafarpour, E. Huang, K. Smith, and F.Bullo, "Flow and elastic networks on the n-torus: geometry, analysis, and computation," 2019, available online at https://arxiv.org/pdf/1901.11189.pdf.

[24] D. Lee, H. D. Nguyen, K. Dvijotham, and K. Turitsyn, "Convex restriction of power flow feasible sets," 2019, available online at https://arxiv.org/pdf/1803.00818.pdf.

[25] V. Chvátal and E. Szemerédi, "Short cycles in directed graphs," *Journal of Combinatorial Theory, Series B*, vol. 35, no. 3, pp. 323–327, 1983.

[26] N. Korneyenko, "Combinatorial algorithms on a class of graphs," *Discrete Applied Mathematics*, vol. 54, pp. 215–217, 1994.

[27] T. S. Developers, "Sagemath, the Sage Mathematics Software System (Version 8.9)," 2019, available online at https://www.sagemath.org.

[28] R. Zimmerman, C. Murillo-Sanchez, and R. Thomas, "Matpower: Steady-state operations, planning and analysis tools for power systems research and education," *IEEE Transactions on Power Systems*, vol. 26, no. 1, pp. 12–19, 2011.

X. Appendix

A. Proof of Lemma 1

proof. The equation for the real power flow from node k to node ℓ over line $\{k,\ell\}$ is given in equation (3). After combining the cosine and sine functions into one sine function, we obtain a simpler equation for both flows:

$$p_{k\ell} = G_{k\ell}|v_k|^2 + |v_k|\cdot|v_\ell|Z_{k\ell}\sin(\theta_{k\ell}+\gamma_{k\ell}) \tag{18}$$

With a simple rearrangement:

$$\sin(\theta_{k\ell}+\gamma_{k\ell}) = \frac{p_{k\ell}-G_{k\ell}|v_k|^2}{|v_k|\cdot|v_\ell|Z_{k\ell}} \tag{19}$$

Using the assumption made on the angle differences and the definition of $\gamma_{k\ell}$, we deduce the following bounds on $\theta_{k\ell}+\gamma_{k\ell}$:

$$\begin{aligned}
&\theta_{k\ell}+\gamma_{k\ell} \geq -\tan^{-1}(B_{k\ell}/G_{k\ell}) + \tan^{-1}(-G_{k\ell}/B_{k\ell})\\
&= -\Big(\frac{\pi}{2} - \tan^{-1}(G_{k\ell}/B_{k\ell})\Big) - \tan^{-1}(G_{k\ell}/B_{k\ell}) = -\frac{\pi}{2}\\
&\theta_{k\ell}+\gamma_{k\ell} \leq \tan^{-1}(B_{k\ell}/G_{k\ell}) + \tan^{-1}(-G_{k\ell}/B_{k\ell})\\
&= \frac{\pi}{2} - 2\tan^{-1}(G_{k\ell}/B_{k\ell}) \leq \frac{\pi}{2}
\end{aligned}$$

In summary, the angle $\theta_{k\ell}+\gamma_{k\ell}$ belongs to the range $[-0.5\pi, 0.5\pi]$ and therefore there exists a unique value of $\theta_{k\ell}+\gamma_{k\ell}$ that satisfies equation (19), leading to a unique value of $\theta_{k\ell}$. To prove the second part of the lemma, recall that the equation for the real power flow from node k to node ℓ over line $\{k,\ell\}$ is given in equation (3). Similarly, the real power flow in the opposite direction (from node ℓ to k) is given by:

$$p_{\ell k} = G_{k\ell}(|v_\ell|^2 - |v_k|\cdot|v_\ell|\cos\theta_{k\ell}) - B_{k\ell}|v_k|\cdot|v_\ell|\sin\theta_{k\ell} \tag{20}$$

After combining the cosine and sine functions into one sine function, we arrive at a simpler equation similar to equation (18):

$$p_{\ell k} = G_{k\ell}|v_\ell|^2 - |v_k|\cdot|v_\ell|Z_{k\ell}\sin(\theta_{k\ell}-\gamma_{k\ell}) \tag{21}$$

Furthermore, we can derive bounds on $\theta_{k\ell}-\gamma_{k\ell}$ similar to those on $\theta_{k\ell}+\gamma_{k\ell}$ shown above:

$$\begin{aligned}
&\theta_{k\ell}-\gamma_{k\ell} \geq -\tan^{-1}(B_{k\ell}/G_{k\ell}) - \tan^{-1}(-G_{k\ell}/B_{k\ell})\\
&= -\frac{\pi}{2} + 2\tan^{-1}(-G_{k\ell}/B_{k\ell}) \geq -\frac{\pi}{2}\\
&\theta_{k\ell}-\gamma_{k\ell} \leq \tan^{-1}(B_{k\ell}/G_{k\ell}) - \tan^{-1}(-G_{k\ell}/B_{k\ell})\\
&= \Big(\frac{\pi}{2} - \tan^{-1}(G_{k\ell}/B_{k\ell})\Big) + \tan^{-1}(G_{k\ell}/B_{k\ell}) = \frac{\pi}{2}
\end{aligned}$$

Therefore, taking note of the fact that $\theta_{k\ell}+\gamma_{k\ell}$ and $\theta_{k\ell}-\gamma_{k\ell}$ are bounded by $[-0.5\pi, 0.5\pi]$, $p_{k\ell}$ and $p_{\ell k}$ are increasing and decreasing functions of $\theta_{k\ell}$, respectively. It can be concluded that $p_{\ell k}$ is a decreasing function of $p_{k\ell}$ for $p_{k\ell} \in (\underline{p}_{k\ell}, \overline{p}_{k\ell})$.

B. Proof of Theorem 2

(a) Let $P \in \mathcal{P}(\mathbb{G}, \Gamma(\mathbb{G}))$. We show by construction that the specification of P uniquely determines $\Theta \in \Gamma(\mathbb{G})$ such that $P = \hat{P}(\Theta)$. Note that since the power system has a tree topology, there is a unique path E_k between any bus k and bus 1 (consisting of successive lines) and that the distance $c(k)$ is therefore well-defined. Let $\overline{c} = \max_{k\in\mathbb{V}} c(k)$. We prove the result by using an induction argument on the decreasing distance $\hat{c}$. That is, the induction starts at $\hat{c} = \overline{c}$ and then considers successively smaller values of $\hat{c}$.

First, consider the case with distance $\hat{c} = \overline{c}$. Consider each bus k with $c(k) = \overline{c}$. Note that each such bus k is a leaf of the tree and that the injection p_k at this bus equals $p_{k\ell}(\theta_{k\ell})$, where $\{k,\ell\} \in \mathbb{T}$ is the unique line connected to bus k and $\theta_{k\ell}$ is the angle difference across this line. By Lemma 1, this means that p_k uniquely determines $\theta_{k\ell}$. Consequently, we can also evaluate $p_{\ell k}(-\theta_{k\ell})$, i.e., the power fow from bus ℓ into the line at the other end.

Now, suppose that for each bus k with $c(k) = \hat{c}$, we have that the injections p_k for each bus $k \in \mathbb{V}\setminus\{1\}$ with $c(k) \geq \hat{c}$ uniquely determines $\theta_{k\ell}$, where $\{k,\ell\} \in \mathbb{T}$ is the unique line connected to bus k such that $c(\ell) = c(k) - 1 = \hat{c} - 1$. Consider any bus k' with $c(k') = \hat{c} - 1$ and suppose that $\{k',\ell'\} \in \mathbb{T}$ is the unique line connected to bus k' such that $c(\ell') = c(k) - 2 = \hat{c} - 2$. By power balance at bus k', $p_{k',\ell'}(\theta_{k',\ell'})$ equals the injection $p_{k'}$ minus the sum of the flows onto each other line $\{k',\ell''\}$ incident to bus k'. However, by assumption, $c(\ell'') \geq \hat{c}$ and so the flow on each such line $\{k',\ell''\}$ is uniquely determined by the injections p_k for each bus with $c(k) \geq \hat{c}$. In turn, this means that the flow $p_{k',\ell'}(\theta_{k'\ell'})$ and the corresponding angle $\theta_{k'\ell'}$ are both uniquely determined by $p_{k'}$ together with the injections p_k for each bus with $c(k) \geq \hat{c}$. That is, the angle $\theta_{k'\ell'}$ and the flow $p_{k',\ell'}(\theta_{k'\ell'})$ are uniquely determined by the injections p_k for each bus with $c(k) \geq \hat{c} - 1$.

The induction continues to the root of the tree; that is, to bus 1. Hence, for all $\{k,\ell\} \in \mathbb{T}$, the injections p_k for each bus $k \in \mathbb{V}$ uniquely determines both $p_{k\ell}(\theta_{k\ell})$ and the corresponding angle $\theta_{k\ell}$ and $p_{\ell k}(-\theta_{k\ell})$. Now, note that the angle $\theta_1 = 0$. Therefore, since each angle difference is uniquely specified, this means that the corresponding angles are also uniquely determined. As a result, there is a unique $\Theta \in \Gamma(\mathbb{G})$ such that $P = \hat{P}(\Theta)$.

(b) Suppose that $P^a, P^b \in \mathcal{P}(\mathbb{G}, \Gamma(\mathbb{G}))$, with the corresponding flows also labeled by superscript a and b, and let $\lambda \in [0,1]$ be given. Let $\Theta^a, \Theta^b \in \Gamma(\mathbb{G})$ be the unique angles satisfying $P^a = \mathcal{P}(\mathbb{G}, \Theta^a)$ and $P^b = \mathcal{P}(\mathbb{G}, \Theta^b)$. Consider the injection $P^\star = \lambda P^a + (1-\lambda)P^b$. To prove convexity of $\mathcal{P}(\mathbb{G}, \Gamma(\mathbb{G}))$, it is enough to show that $P^\star \in \mathcal{P}(\mathbb{G}, \Gamma(\mathbb{G}))$, which will involve constructing an angle $\Theta^\star \in \Gamma(\mathbb{G})$ such that $P^\star = \mathcal{P}(\mathbb{G}, \Theta^\star)$. By a similar argument to Part 1, first consider injections at buses k with $c(k) = \overline{c}$ and let $\{k,\ell\} \in \mathbb{T}$ be the unique line connected to bus k. Note that, by definition, $P^\star_k = \lambda P^a_k + (1-\lambda)P^b_k$ and therefore the corresponding flow $p^\star_{k\ell}$ is the convex combination of the corresponding injections. In other words,

$$\begin{aligned}
p^\star_{k\ell} &= P^\star_k\\
&= \lambda P^a_k + (1-\lambda)P^b_k, \text{ by definition of } P^\star_k,\\
&= \lambda p_{k\ell}(\theta^a_{k\ell}) + (1-\lambda)p_{k\ell}(\theta^b_{k\ell})
\end{aligned}$$

The first and third equations come from the fact that $\{k,\ell\} \in \mathbb{T}$ is the unique line connected to bus k. Now, note that the values of flows $p_{k\ell}(\theta^a_{k\ell})$ and $p_{k\ell}(\theta^b_{k\ell})$ belong to $[\underline{p}_{k\ell}, \overline{p}_{k\ell}]$, which is a convex set. Thus, we also have that $p^\star_{k\ell} \in [\underline{p}_{k\ell}, \overline{p}_{k\ell}]$.

Therefore, there exists a unique $|\theta^\star_{k\ell}|\leq \tan^{-1}(B_{k\ell}/G_{k\ell})$ such that $p^\star_{k\ell} = p_{k\ell}(\theta^\star_{k\ell})$. We proceed as in Part 1 by using an induction argument on the decreasing distance $\hat{c}$. That is, the induction starts at $\hat{c}$ and shows that for each $\{k,\ell\} \in \mathbb{T}$, the corresponding angle difference $\theta^\star_{k\ell}$ with injections $P^\star$ satisfies $|\theta^\star_{k\ell}|\leq \tan^{-1}(B_{k\ell}/G_{k\ell})$. Proceeding to bus 1, and again noting that $\theta_1 = 0$ is specified, it can be concluded that there is a uniquely defined $\Theta^\star \in \Gamma(\mathbb{G})$ such that $P^\star = \mathcal{P}(\mathbb{G}, \Theta^\star)$. Therefore, $\mathcal{P}(\mathbb{G}, \Gamma(\mathbb{G}))$ is convex.

C. Lemma 9 and its proof

For each pair of vertices $k, \ell \in \mathbb{V}$, we define $\hat{\Theta}_{k\ell} = \hat{\Theta}_k - \hat{\Theta}_\ell$. Note that we do not require that $\{k,\ell\} \in \mathbb{T}$ in the definition of $\hat{\Theta}_{k\ell}$ and in the next lemma:

Lemma 9. *Suppose that the power system $\mathbb{G} = (\mathbb{V}, \mathbb{T})$ has a tree topology. Then, for each $k \in \mathbb{V} \setminus \{1\}$ and $\ell \in \mathbb{V}$ and for each $P \in \mathcal{P}(\mathbb{G}, \Gamma(\mathbb{G}))$, we have $\frac{\partial \hat{\Theta}_{k\ell}}{\partial p_k}(P) \geq 0$.*

proof. Consider the path E_k from bus k to bus 1 and the path E_ℓ from bus ℓ to bus 1. Note that $\hat{\Theta}_k = \sum_{(k',\ell')\in E_k} \hat{\Theta}_{k'\ell'}$ and $\hat{\Theta}_\ell = \sum_{(k',\ell')\in E_\ell} \hat{\Theta}_{k'\ell'}$, because $\theta_1 = 0$. Moreover, $\hat{\Theta}_{k\ell} = \sum_{(k',\ell')\in E_k} \hat{\Theta}_{k'\ell'} - \sum_{(k',\ell')\in E_\ell} \hat{\Theta}_{k'\ell'}$. Now, observe that changes in injection at bus k can only affect flows, and therefore angle differences, in the path between bus k and bus 1. Moreover, changes in flows and angles differences in the common part of the path $E_k \cap E_\ell$ affect the angle at both buses k and ℓ equally. Define $E_{k\ell} = E_k \setminus (E_k \cap E_\ell)$. That is, $E_{k\ell}$ is the path from bus k to the bus that is common to both E_k and E_ℓ and furthest from bus 1. Then:

$$\frac{\partial \hat{\Theta}_{k\ell}}{\partial p_k}(P) = \sum_{(k',\ell')\in E_{k\ell}} \frac{\partial \hat{\Theta}_{k'\ell'}}{\partial p_k}(P).$$

We now observe that the relationship between injection at bus k and angle differences at lines in this path $E_{k\ell}$ are all monotonic. That is, $\frac{\partial \hat{\Theta}_{k\ell}}{\partial p_k}(P) \geq 0$. According to Lemma 9, we can see that the angle difference between any non-slack bus k and any other bus ℓ is a monotonically increasing function of the real power injection at bus k when the injection vector P is within the *set of allowable injections*.

D. Proof of Lemma 3

Suppose that there are two distinct vectors of voltage angles, $\Theta^*, \Theta^{**} \in \Gamma(\mathbb{G})$ that satisfy the power flow equations. Without loss of generality, assume that $\theta^{**}_{12} > \theta^*_{12}$. Then, due to power balance at buses $2, \ldots, N$ and Assumption 1, a simple induction argument shows that

$$\theta^{**}_{i,i+1} - \theta^*_{i,i+1} > 0 \quad \forall i = \{1, \ldots, N\}, \tag{22}$$

where bus $N+1$ is again bus 1. Furthermore, we have that

$$\theta^{**}_{i,i+1} - \theta^*_{i,i+1} < \pi \quad \forall i = \{1, \ldots, N\}, \tag{23}$$

which can be shown using the same logic followed to derive equation (27). Finally, by definition,

$$\theta^{**}_{1,N} - \theta^*_{1,N} = \sum_{i=1}^{N-1} (\theta^{**}_{i,i+1} - \theta^*_{i,i+1}) > 0 \tag{24}$$

and also,

$$\begin{aligned}\theta^{**}_{1,N} - \theta^*_{1,N} &= \sum_{i=1}^{N-1} (\theta^{**}_{i,i+1} - \theta^*_{i,i+1}) \leq \sum_{i=1}^{N-1} |\theta^{**}_{i,i+1} - \theta^*_{i,i+1}| \\ &\leq \sum_{i=1}^{N-1} (|\theta^{**}_{i,i+1}|+|\theta^*_{i,i+1}|) \\ &< \sum_{i=1}^{N-1} \omega^{**}_{i,i+1} + \sum_{i=1}^{N-1} \omega^*_{i,i+1} < \pi.\end{aligned}$$

This is a contradiction to equation (23) and therefore there cannot be two distinct solutions.

E. Proof of Theorem 4

In order to prove by contraction, suppose that there are two distinct solutions to the power flow problem, denoted as $\Theta^*, \Theta^{**} \in \Gamma(\mathbb{G})$. Now, we define a digraph $\mathbb{D}^r(\mathbb{G}) = \mathbb{D}^r(\mathbb{V}, \mathbb{A}^r)$ where the direction of each directed edge in $\mathbb{A}^r$ is based on the difference (residual) between these two solutions. Hereby, we define the residual incidence matrix L^r for $\mathbb{D}^r(\mathbb{G})$ below:

$$L^r(a,k) = \begin{cases} -1 & \text{if } a = (k,\ell) \in \mathbb{A}^r \text{ and } \theta^{**}_{k,\ell} > \theta^*_{k,\ell} \\ 1 & \text{if } a = (\ell,k) \in \mathbb{A}^r \text{ and } \theta^{**}_{k,\ell} > \theta^*_{k,\ell} \\ 1 & \text{if } a = (k,\ell) \in \mathbb{A}^r \text{ and } \theta^{**}_{k,\ell} < \theta^*_{k,\ell} \\ -1 & \text{if } a = (\ell,k) \in \mathbb{A}^r \text{ and } \theta^{**}_{k,\ell} < \theta^*_{k,\ell} \end{cases} \tag{25}$$

Note that because of power balance at each node, this orientation has to be a *Feasible Orientation*. By assumption, for this fixed feasible orientation $\mathbb{D}^r(\mathbb{G}) \in \mathcal{D}_f(\mathbb{G})$, there exists a directed cycle $\mathbb{C}$ satisfying the inequality in (8). Without loss of generality, assume that $\theta^{**}_{u(1),u(2)} > \theta^*_{u(1),u(2)}$. Then, because $\mathbb{C}$ is a directed cycle, it holds that

$$\theta^{**}_{u(i),u(i+1)} - \theta^*_{u(i),u(i+1)} > 0 \quad \forall i = \{1, \ldots, N\}, \tag{26}$$

where the $(N+1)^{\text{th}}$ bus is again the 1^{st} bus. Furthermore,

$$\theta^{**}_{u(i),u(i+1)} - \theta^*_{u(i),u(i+1)} < \pi \quad \forall i = \{1, \ldots, N\}, \tag{27}$$

which is due to the following inequalities:

$$\begin{aligned}\theta^{**}_{u(i),u(i+1)} - \theta^*_{u(i),u(i+1)} &\leq |\theta^{**}_{u(i),u(i+1)} - \theta^*_{u(i),u(i+1)}| \\ &\leq |\theta^{**}_{u(i),u(i+1)}|+|\theta^*_{u(i),u(i+1)}| < 2 \cdot \omega_{u(i),u(i+1)} < \pi\end{aligned}$$

However, by definition,

$$\begin{aligned}&\theta^{**}_{u(1),u(N)} - \theta^*_{u(1),u(N)} = \sum_{i=1}^{N-1} (\theta^{**}_{u(i),u(i+1)} - \theta^*_{u(i),u(i+1)}) \\ &\leq \sum_{i=1}^{N-1} |\theta^{**}_{u(i),u(i+1)} - \theta^*_{u(i),u(i+1)}| \\ &\leq \sum_{i=1}^{N-1} |\theta^{**}_{u(i),u(i+1)}|+ \sum_{i=1}^{N-1} |\theta^*_{u(i),u(i+1)}| \\ &< \sum_{i=1}^{N-1} \omega_{u(i),u(i+1)} + \sum_{i=1}^{N-1} \omega_{u(i),u(i+1)} < \pi\end{aligned}$$

which is a contradiction to equations (26) and (27). Therefore, there cannot be two distinct vectors $\Theta^*, \Theta^{**} \in \Gamma(\mathbb{G})$ that satisfy $P = \hat{P}(\Theta)$.

F. Proof of Theorem 5

Suppose that equation (10) is satisfied. In other words, to restate the equation here,

$$\omega_{k\ell} < \frac{\pi}{2\cdot(\Delta(\mathbb{G})-1)} \quad \forall\{k,\ell\}\in\mathbb{E}. \tag{28}$$

Defining $\omega_{k\ell}^{max} = \max_{\{k,\ell\}\in\mathbb{E}} \omega_{k\ell}$, we also have that

$$\omega_{k\ell}^{max} < \frac{\pi}{2\cdot(\Delta(\mathbb{G})-1)} \quad \forall\{k,\ell\}\in\mathbb{E}. \tag{29}$$

Multiplying both sides of the equation by $(\Delta(\mathbb{G})-1)$ yields

$$(\Delta(\mathbb{G})-1)\cdot\omega_{k\ell}^{max} < \frac{\pi}{2}. \tag{30}$$

Now, using the definition of $\Delta(\mathbb{G})$, the following holds true for every $\mathbb{D}\in\mathcal{D}_f(\mathbb{G})$:

$$(\delta(\mathbb{D})-1)\cdot\omega_{k\ell}^{max} < \frac{\pi}{2}. \tag{31}$$

Since $\delta(\mathbb{D})$ represents the length of the smallest directed cycle of $\mathbb{D}$, let us denote this smallest directed cycle by $\mathbb{C}$ and its vertex set by $\mathbb{V}_{dc} = \{u(1),\ldots,u(|\mathbb{V}_{dc}|)\} \subseteq \mathbb{V}$. Then, the above inequality becomes equivalent to the following:

$$(|\mathbb{V}_{dc}|-1)\cdot\omega_{k\ell}^{max} < \frac{\pi}{2}. \tag{32}$$

This implies that

$$\sum_{i=1}^{|\mathbb{V}_{dc}|-1} \omega_{u(i),u(i+1)} < \frac{\pi}{2}. \tag{33}$$

Therefore, we have satisfied condition (8) of Theorem 4 and as a result can conclude that for each $P\in\mathcal{P}(\mathbb{G},\Gamma(\mathbb{G}))$ there cannot be multiple distinct solutions for the $P=\hat{P}(\Theta)$ problem.

G. Lemma 10 and its proof

Lemma 10. *For a given graph $\mathbb{G}=(\mathbb{V},\mathbb{E})$, the following inequality holds:*

$$\Delta(\mathbb{G}) \le \kappa(\mathbb{G}) \tag{34}$$

Proof. Consider an arbitrary *feasible orientation* on graph $\mathbb{G}$, and denote it as $\mathbb{D}=(\mathbb{V},\mathbb{A})$. We will first show that the shortest directed cycle in $\mathbb{D}$ must by chordless. Recall that because the feasible orientation enforces every vertex to have at least one incoming arc and one outgoing arc, there always exists a sequence of arcs in $\mathbb{D}$ that form a directed cycle. To put this in another way, there is at least one directed cycle in $\mathbb{D}(\mathbb{G})$. Let us call the shortest of these directed cycles, $\mathbb{C}^0$ and denote its vertices using the ordered set $\{u(1),\ldots,u(N)\}$. In other words, $(u(i),u(i+1))\in\mathbb{A}\ \forall i\in\{1,\ldots,N-1\}$ and $(u(N),u(1))\in\mathbb{A}$. In order to prove by contradiction, assume that $\mathbb{C}^0$ contains a chord with two endpoints $u(k)$, $u(\ell)$ and $k<\ell$. Then, this chord divides $\mathbb{C}^0$ into two cycles $\mathbb{C}^1$ and $\mathbb{C}^2$ such that the symmetric difference of the two becomes $\mathbb{C}^0$. Depending on whether $(u(k),u(\ell))\in\mathbb{A}$ or $(u(\ell),u(k))\in\mathbb{A}$, exactly one of $\mathbb{C}^1$ and $\mathbb{C}^2$ again becomes a directed cycle. This is a contradiction to $\mathbb{C}^0$ being the shortest directed cycle. So far, we have established that the shortest directed cycle of a given digraph is a chordless cycle of its underlying undirected graph $\mathbb{G}$. It follows naturally that the length of this shortest directed cycle is less than the length of the longest chordless cycle in $\mathbb{G}$:

$$\delta(\mathbb{D}) \le \kappa(\mathbb{G}) \text{ for any } \mathbb{D}\in\mathcal{D}_f(\mathbb{G})$$

Taking the maximum over $\mathbb{D}\in\mathcal{D}_f(\mathbb{G})$ on both sides of the inequality and using the definition of *maximal girth* in (9), we arrive at the desired conclusion.

H. Proof of Theorem 6

(a) Consider a graph $\mathbb{G}=(\mathbb{V},\mathbb{E},\mathbb{W})$ with a dangling vertex k. See Figure 10 for an example, where $k=1$ is the dangling vertex. By definition, vertex k cannot be part of any cycle. Therefore, if there exists a directed cycle $\mathbb{C}$ that satisfies condition (10) for $\mathbb{G}^r = (\bar{\mathbb{V}},\bar{\mathbb{E}},\bar{\mathbb{W}})$, the same cycle also satisfies condition (10) for $\mathbb{G}=(\mathbb{V},\mathbb{E},\mathbb{W})$.

(b) Consider a graph $\mathbb{G}=(\mathbb{V},\mathbb{E},\mathbb{W})$ with a highway-path. See Figure 11 for an example, where the vertex set $\{1,2,3,4\}$ specify the highway-path. Denote the vertex set of the highway-path $\mathbb{P}$ as the following:

$$\mathbb{V}^h = \{s,u^h(1),u^h(2),\ldots,u^h(H),t\} \tag{35}$$

For $\mathbb{G}^r = (\bar{\mathbb{V}},\bar{\mathbb{E}},\bar{\mathbb{W}})$, suppose that condition (10) is satisfied for a directed cycle $\mathbb{C}^r$ that includes the edge $\{s,t\}$. This implies that for $\mathbb{G}=(\mathbb{V},\mathbb{E},\mathbb{W})$, condition (10) is satisfied for a directed cycle $\mathbb{C}$ that includes the edges $\{s,u^h(1)\},\{u^h(1),u^h(2)\},\ldots,\{u^h(H-1),u^h(H)\}$ and $\{u^h(H),t\}$. This is because the edges in a highway-path must either all be part of a cycle or all not be part of any cycle.

(c) Consider a graph $\mathbb{G}=(\mathbb{V},\mathbb{E},\mathbb{W})$ with a pair of parallel edges e_1 and e_2, both connecting the two end-points s and t. For $\mathbb{G}^r = (\bar{\mathbb{V}},\bar{\mathbb{E}},\bar{\mathbb{W}})$, suppose that condition (10) is satisfied for a directed cycle $\mathbb{C}^r$ that includes the edge $\{s,t\}$. This implies that for $\mathbb{G}=(\mathbb{V},\mathbb{E},\mathbb{W})$, condition (10) is satisfied for a directed cycle $\mathbb{C}$ that either (i) includes only edge e_1 but not e_2, (ii) includes only edge e_2 but not e_1, or (iii) includes both edges e_1 and e_2.

I. Proof of Theorem 8

We prove that there is a linear-time algorithm by construction. Denote the vertex set of the auxiliary path of the j^{th} outer-cycle by:

$$\mathbb{V}_j^a = \{s_j,u_j^a(1),u_j^a(2),\ldots,u_j^a(N_j),t_j\}$$

Set the *primary flow* to be $p(s_j,u_j^a(1))$ and initialize its value to be the average-value of the range $[\underline{p}(s_j,u_j^a(1)),\bar{p}(s_j,u_j^a(1))]$. Here, we again abuse some notation so that $p(k,\ell)$ denotes the real power flow from vertex k to ℓ. Then, because all of the intermediate nodes $u_j^a(1),\ldots,u_j^a(N_j)$ have degree two, the subsequent flows on the auxiliary path can be calculated by simple arithmetic. Furthermore, due to the *allowable angle* assumption, we can uniquely determine the angle difference across every edge that is part of the auxiliary path. Summing them up will also provide the value for θ_{s_j,t_j}. Also, because of the assumption made in (17), the principal path consists of a single edge. The flow on this edge can be calculated by using the previously calculated $\theta s_j, t_j$. Finally, note that the flows that we calculated so far are all increasing functions of the *primary flow*. This process can be repeated for all outer-cycles in $\mathcal{O}$ until the last cycle $\mathbb{C}_R$. For $\mathbb{C}_R$, instead of calculating θ_{s_R,t_R} and then using it to calculate $p(s_R, t_R)$, do the following: $p(s_R, t_R) = p_{t_R} - p(u_R(N_R), t_R)$. Finally, calculate all the angle differences using these flow values and add them around the cycle. If the angle sum is greater than zero, reduce the range of the *primary flow* to $[\underline{p}(s_j, u_j^a(1)), p(s_j, u_j^a(1))]$ and restart the process; otherwise, if the angle sum is greater than zero, reduce the range of the *primary flow* to $[p(s_j, u_j^a(1)), \bar{p}(s_j, u_j^a(1))]$ and restart the process. We repeat this process until the range is less than ϵ. Calculating all flows takes $O(|\mathbb{E}|)$ time and this is repeated for $log(1/\epsilon)$ times if we want ϵ-accuracy. This concludes the proof.

J. Additional Figures

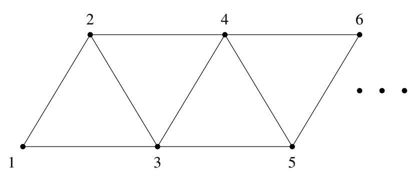

Fig. 9: A test network consisting of triangles

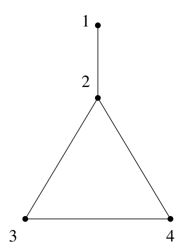

Fig. 10: A simple graph with dangling vertex

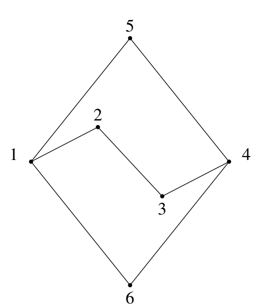

Fig. 11: A simple graph with multiple edges in series